

# INTRINSIC ENTROPY OF CONTEXT LENGTH SCALING IN LLMS

000  
001  
002  
003  
004  
005 **Anonymous authors**  
006 Paper under double-blind review  
007  
008  
009  
010  
011  
012  
013  
014  
015  
016  
017  
018  
019  
020  
021  
022  
023  
024  
025  
026  
027  
028  
029  
030  
031  
032  
033  
034  
035  
036  
037  
038  
039  
040  
041  
042  
043  
044  
045  
046  
047  
048  
049  
050  
051  
052  
053  
054  
055  
056  
057  
058  
059  
060  
061  
062  
063  
064  
065  
066  
067  
068  
069  
070  
071  
072  
073  
074  
075  
076  
077  
078  
079  
080  
081  
082  
083  
084  
085  
086  
087  
088  
089  
090  
091  
092  
093  
094  
095  
096  
097  
098  
099  
100  
101  
102  
103  
104  
105  
106  
107  
108  
109  
110  
111  
112  
113  
114  
115  
116  
117  
118  
119  
120  
121  
122  
123  
124  
125  
126  
127  
128  
129  
130  
131  
132  
133  
134  
135  
136  
137  
138  
139  
140  
141  
142  
143  
144  
145  
146  
147  
148  
149  
150  
151  
152  
153  
154  
155  
156  
157  
158  
159  
160  
161  
162  
163  
164  
165  
166  
167  
168  
169  
170  
171  
172  
173  
174  
175  
176  
177  
178  
179  
180  
181  
182  
183  
184  
185  
186  
187  
188  
189  
190  
191  
192  
193  
194  
195  
196  
197  
198  
199  
200  
201  
202  
203  
204  
205  
206  
207  
208  
209  
210  
211  
212  
213  
214  
215  
216  
217  
218  
219  
220  
221  
222  
223  
224  
225  
226  
227  
228  
229  
230  
231  
232  
233  
234  
235  
236  
237  
238  
239  
240  
241  
242  
243  
244  
245  
246  
247  
248  
249  
250  
251  
252  
253  
254  
255  
256  
257  
258  
259  
260  
261  
262  
263  
264  
265  
266  
267  
268  
269  
270  
271  
272  
273  
274  
275  
276  
277  
278  
279  
280  
281  
282  
283  
284  
285  
286  
287  
288  
289  
290  
291  
292  
293  
294  
295  
296  
297  
298  
299  
300  
301  
302  
303  
304  
305  
306  
307  
308  
309  
310  
311  
312  
313  
314  
315  
316  
317  
318  
319  
320  
321  
322  
323  
324  
325  
326  
327  
328  
329  
330  
331  
332  
333  
334  
335  
336  
337  
338  
339  
340  
341  
342  
343  
344  
345  
346  
347  
348  
349  
350  
351  
352  
353  
354  
355  
356  
357  
358  
359  
360  
361  
362  
363  
364  
365  
366  
367  
368  
369  
370  
371  
372  
373  
374  
375  
376  
377  
378  
379  
380  
381  
382  
383  
384  
385  
386  
387  
388  
389  
390  
391  
392  
393  
394  
395  
396  
397  
398  
399  
400  
401  
402  
403  
404  
405  
406  
407  
408  
409  
410  
411  
412  
413  
414  
415  
416  
417  
418  
419  
420  
421  
422  
423  
424  
425  
426  
427  
428  
429  
430  
431  
432  
433  
434  
435  
436  
437  
438  
439  
440  
441  
442  
443  
444  
445  
446  
447  
448  
449  
450  
451  
452  
453  
454  
455  
456  
457  
458  
459  
460  
461  
462  
463  
464  
465  
466  
467  
468  
469  
470  
471  
472  
473  
474  
475  
476  
477  
478  
479  
480  
481  
482  
483  
484  
485  
486  
487  
488  
489  
490  
491  
492  
493  
494  
495  
496  
497  
498  
499  
500  
501  
502  
503  
504  
505  
506  
507  
508  
509  
510  
511  
512  
513  
514  
515  
516  
517  
518  
519  
520  
521  
522  
523  
524  
525  
526  
527  
528  
529  
530  
531  
532  
533  
534  
535  
536  
537  
538  
539  
540  
541  
542  
543  
544  
545  
546  
547  
548  
549  
550  
551  
552  
553  
554  
555  
556  
557  
558  
559  
559  
560  
561  
562  
563  
564  
565  
566  
567  
568  
569  
569  
570  
571  
572  
573  
574  
575  
576  
577  
578  
579  
579  
580  
581  
582  
583  
584  
585  
586  
587  
588  
589  
589  
590  
591  
592  
593  
594  
595  
596  
597  
598  
599  
599  
600  
601  
602  
603  
604  
605  
606  
607  
608  
609  
609  
610  
611  
612  
613  
614  
615  
616  
617  
618  
619  
619  
620  
621  
622  
623  
624  
625  
626  
627  
628  
629  
629  
630  
631  
632  
633  
634  
635  
636  
637  
638  
639  
639  
640  
641  
642  
643  
644  
645  
646  
647  
648  
649  
649  
650  
651  
652  
653  
654  
655  
656  
657  
658  
659  
659  
660  
661  
662  
663  
664  
665  
666  
667  
668  
669  
669  
670  
671  
672  
673  
674  
675  
676  
677  
678  
679  
679  
680  
681  
682  
683  
684  
685  
686  
687  
688  
689  
689  
690  
691  
692  
693  
694  
695  
696  
697  
698  
699  
699  
700  
701  
702  
703  
704  
705  
706  
707  
708  
709  
709  
710  
711  
712  
713  
714  
715  
716  
717  
718  
719  
719  
720  
721  
722  
723  
724  
725  
726  
727  
728  
729  
729  
730  
731  
732  
733  
734  
735  
736  
737  
738  
739  
739  
740  
741  
742  
743  
744  
745  
746  
747  
748  
749  
749  
750  
751  
752  
753  
754  
755  
756  
757  
758  
759  
759  
760  
761  
762  
763  
764  
765  
766  
767  
768  
769  
769  
770  
771  
772  
773  
774  
775  
776  
777  
778  
779  
779  
780  
781  
782  
783  
784  
785  
786  
787  
788  
789  
789  
790  
791  
792  
793  
794  
795  
796  
797  
798  
799  
799  
800  
801  
802  
803  
804  
805  
806  
807  
808  
809  
809  
810  
811  
812  
813  
814  
815  
816  
817  
818  
819  
819  
820  
821  
822  
823  
824  
825  
826  
827  
828  
829  
829  
830  
831  
832  
833  
834  
835  
836  
837  
838  
839  
839  
840  
841  
842  
843  
844  
845  
846  
847  
848  
849  
849  
850  
851  
852  
853  
854  
855  
856  
857  
858  
859  
859  
860  
861  
862  
863  
864  
865  
866  
867  
868  
869  
869  
870  
871  
872  
873  
874  
875  
876  
877  
878  
879  
879  
880  
881  
882  
883  
884  
885  
886  
887  
888  
889  
889  
890  
891  
892  
893  
894  
895  
896  
897  
898  
899  
899  
900  
901  
902  
903  
904  
905  
906  
907  
908  
909  
909  
910  
911  
912  
913  
914  
915  
916  
917  
918  
919  
919  
920  
921  
922  
923  
924  
925  
926  
927  
928  
929  
929  
930  
931  
932  
933  
934  
935  
936  
937  
938  
939  
939  
940  
941  
942  
943  
944  
945  
946  
947  
948  
949  
949  
950  
951  
952  
953  
954  
955  
956  
957  
958  
959  
959  
960  
961  
962  
963  
964  
965  
966  
967  
968  
969  
969  
970  
971  
972  
973  
974  
975  
976  
977  
978  
979  
979  
980  
981  
982  
983  
984  
985  
986  
987  
988  
989  
989  
990  
991  
992  
993  
994  
995  
996  
997  
998  
999  
1000  
1001  
1002  
1003  
1004  
1005  
1006  
1007  
1008  
1009  
1009  
1010  
1011  
1012  
1013  
1014  
1015  
1016  
1017  
1018  
1019  
1019  
1020  
1021  
1022  
1023  
1024  
1025  
1026  
1027  
1028  
1029  
1030  
1031  
1032  
1033  
1034  
1035  
1036  
1037  
1038  
1039  
1039  
1040  
1041  
1042  
1043  
1044  
1045  
1046  
1047  
1048  
1049  
1049  
1050  
1051  
1052  
1053  
1054  
1055  
1056  
1057  
1058  
1059  
1059  
1060  
1061  
1062  
1063  
1064  
1065  
1066  
1067  
1068  
1069  
1069  
1070  
1071  
1072  
1073  
1074  
1075  
1076  
1077  
1078  
1079  
1079  
1080  
1081  
1082  
1083  
1084  
1085  
1086  
1087  
1088  
1089  
1089  
1090  
1091  
1092  
1093  
1094  
1095  
1096  
1097  
1098  
1098  
1099  
1099  
1100  
1101  
1102  
1103  
1104  
1105  
1106  
1107  
1108  
1109  
1109  
1110  
1111  
1112  
1113  
1114  
1115  
1116  
1117  
1118  
1119  
1119  
1120  
1121  
1122  
1123  
1124  
1125  
1126  
1127  
1128  
1129  
1129  
1130  
1131  
1132  
1133  
1134  
1135  
1136  
1137  
1138  
1139  
1139  
1140  
1141  
1142  
1143  
1144  
1145  
1146  
1147  
1148  
1149  
1149  
1150  
1151  
1152  
1153  
1154  
1155  
1156  
1157  
1158  
1159  
1159  
1160  
1161  
1162  
1163  
1164  
1165  
1166  
1167  
1168  
1169  
1169  
1170  
1171  
1172  
1173  
1174  
1175  
1176  
1177  
1178  
1179  
1179  
1180  
1181  
1182  
1183  
1184  
1185  
1186  
1187  
1188  
1189  
1189  
1190  
1191  
1192  
1193  
1194  
1195  
1196  
1197  
1198  
1198  
1199  
1199  
1200  
1201  
1202  
1203  
1204  
1205  
1206  
1207  
1208  
1209  
1209  
1210  
1211  
1212  
1213  
1214  
1215  
1216  
1217  
1218  
1219  
1219  
1220  
1221  
1222  
1223  
1224  
1225  
1226  
1227  
1228  
1229  
1229  
1230  
1231  
1232  
1233  
1234  
1235  
1236  
1237  
1238  
1239  
1239  
1240  
1241  
1242  
1243  
1244  
1245  
1246  
1247  
1248  
1249  
1249  
1250  
1251  
1252  
1253  
1254  
1255  
1256  
1257  
1258  
1259  
1259  
1260  
1261  
1262  
1263  
1264  
1265  
1266  
1267  
1268  
1269  
1269  
1270  
1271  
1272  
1273  
1274  
1275  
1276  
1277  
1278  
1279  
1279  
1280  
1281  
1282  
1283  
1284  
1285  
1286  
1287  
1288  
1289  
1289  
1290  
1291  
1292  
1293  
1294  
1295  
1296  
1297  
1298  
1298  
1299  
1299  
1300  
1301  
1302  
1303  
1304  
1305  
1306  
1307  
1308  
1309  
1309  
1310  
1311  
1312  
1313  
1314  
1315  
1316  
1317  
1318  
1319  
1319  
1320  
1321  
1322  
1323  
1324  
1325  
1326  
1327  
1328  
1329  
1329  
1330  
1331  
1332  
1333  
1334  
1335  
1336  
1337  
1338  
1339  
1339  
1340  
1341  
1342  
1343  
1344  
1345  
1346  
1347  
1348  
1349  
1349  
1350  
1351  
1352  
1353  
1354  
1355  
1356  
1357  
1358  
1359  
1359  
1360  
1361  
1362  
1363  
1364  
1365  
1366  
1367  
1368  
1369  
1369  
1370  
1371  
1372  
1373  
1374  
1375  
1376  
1377  
1378  
1379  
1379  
1380  
1381  
1382  
1383  
1384  
1385  
1386  
1387  
1388  
1389  
1389  
1390  
1391  
1392  
1393  
1394  
1395  
1396  
1397  
1398  
1398  
1399  
1399  
1400  
1401  
1402  
1403  
1404  
1405  
1406  
1407  
1408  
1409  
1409  
1410  
1411  
1412  
1413  
1414  
1415  
1416  
1417  
1418  
1419  
1419  
1420  
1421  
1422  
1423  
1424  
1425  
1426  
1427  
1428  
1429  
1429  
1430  
1431  
1432  
1433  
1434  
1435  
1436  
1437  
1438  
1439  
1439  
1440  
1441  
1442  
1443  
1444  
1445  
1446  
1447  
1448  
1449  
1449  
1450  
1451  
1452  
1453  
1454  
1455  
1456  
1457  
1458  
1459  
1459  
1460  
1461  
1462  
1463  
1464  
1465  
1466  
1467  
1468  
1469  
1469  
1470  
1471  
1472  
1473  
1474  
1475  
1476  
1477  
1478  
1479  
1479  
1480  
1481  
1482  
1483  
1484  
1485  
1486  
1487  
1488  
1489  
1489  
1490  
1491  
1492  
1493  
1494  
1495  
1496  
1497  
1498  
1498  
1499  
1499  
1500  
1501  
1502  
1503  
1504  
1505  
1506  
1507  
1508  
1509  
1509  
1510  
1511  
1512  
1513  
1514  
1515  
1516  
1517  
1518  
1519  
1519  
1520  
1521  
1522  
1523  
1524  
1525  
1526  
1527  
1528  
1529  
1529  
1530  
1531  
1532  
1533  
1534  
1535  
1536  
1537  
1538  
1539  
1539  
1540  
1541  
1542  
1543  
1544  
1545  
1546  
1547  
1548  
1549  
1549  
1550  
1551  
1552  
1553  
1554  
1555  
1556  
1557  
1558  
1559  
1559  
1560  
1561  
1562  
1563  
1564  
1565  
1566  
1567  
1568  
1569  
1569  
1570  
1571  
1572  
1573  
1574  
1575  
1576  
1577  
1578  
1579  
1579  
1580  
1581  
1582  
1583  
1584  
1585  
1586  
1587  
1588  
1589  
1589  
1590  
1591  
1592  
1593  
1594  
1595  
1596  
1597  
1598  
1598  
1599  
1599  
1600  
1601  
1602  
1603  
1604  
1605  
1606  
1607  
1608  
1609  
1609  
1610  
1611  
1612  
1613  
1614  
1615  
1616  
1617  
1618  
1619  
1619  
1620  
1621  
1622  
1623  
1624  
1625  
1626  
1627  
1628  
1629  
1629  
1630  
1631  
1632  
1633  
1634  
1635  
1636  
1637  
1638  
1639  
1639  
1640  
1641  
1642  
1643  
1644  
1645  
1646  
1647  
1648  
1649  
1649  
1650  
1651  
1652  
1653  
1654  
1655  
1656  
1657  
1658  
1659  
1659  
1660  
1661  
1662  
1663  
1664  
1665  
1666  
1667  
1668  
1669  
1669  
1670  
1671  
1672  
1673  
1674  
1675  
1676  
1677  
1678  
1679  
1679  
1680  
1681  
1682  
1683  
1684  
1685  
1686  
1687  
1688  
1689  
1689  
1690  
1691  
1692  
1693  
1694  
1695  
1696  
1697  
1698  
1698  
1699  
1699  
1700  
1701  
1702  
1703  
1704  
1705  
1706  
1707  
1708  
1709  
1709  
1710  
1711  
1712  
1713  
1714  
1715  
1716  
1717  
1718  
1719  
1719  
1720  
1721  
1722  
1723  
1724  
1725  
1726  
1727  
1728  
1729  
1729  
1730  
1731  
1732  
1733  
1734  
1735  
1736  
1737  
1738  
1739  
1739  
1740  
1741  
1742  
1743  
1744  
1745  
1746  
1747  
1748  
1749  
1749  
1750  
1751  
1752  
1753  
1754  
1755  
1756  
1757  
1758  
1759  
1759  
1760  
1761  
1762  
1763  
1764  
1765  
1766  
1767  
1768  
1769  
1769  
1770  
1771  
1772  
1773  
1774  
1775  
1776  
1777  
1778  
1779  
1779  
1780  
1781  
1782  
1783  
1784  
1785  
1786  
1787  
1788  
1789  
1789  
1790  
1791  
1792  
1793  
1794  
1795  
1796  
1797  
1798  
1798  
1799  
1799  
1800  
1801  
1802  
1803  
1804  
1805  
1806  
1807  
1808  
1809  
1809  
1810  
1811  
1812  
1813  
1814  
1815  
1816  
1817  
1818  
1819  
1819  
1820  
1821  
1822  
1823  
1824  
1825  
1826  
1827  
1828  
1829  
1829  
1830  
1831  
1832  
1833  
1834  
1835  
1836  
1837  
1838  
1839  
1839  
1840  
1841  
1842  
1843  
1844  
1845  
1846  
1847  
1848  
1849  
1849  
1850  
1851  
1852  
1853  
1854  
1855  
1856  
1857  
1858  
1859  
1859  
1860  
1861  
1862  
1863  
1864  
1865  
1866  
1867  
1868  
1869  
1869  
1870  
1871  
1872  
1873  
1874  
1875  
1876  
1877  
1878  
1879  
1879  
1880  
1881  
1882  
1883  
1884  
1885  
1886  
1887  
1888  
1889  
1889  
1890  
1891  
1892  
1893  
1894  
1895  
1896  
1897  
1898  
1898  
1899  
1899  
1900  
1901  
1902  
1903  
1904  
1905  
1906  
190

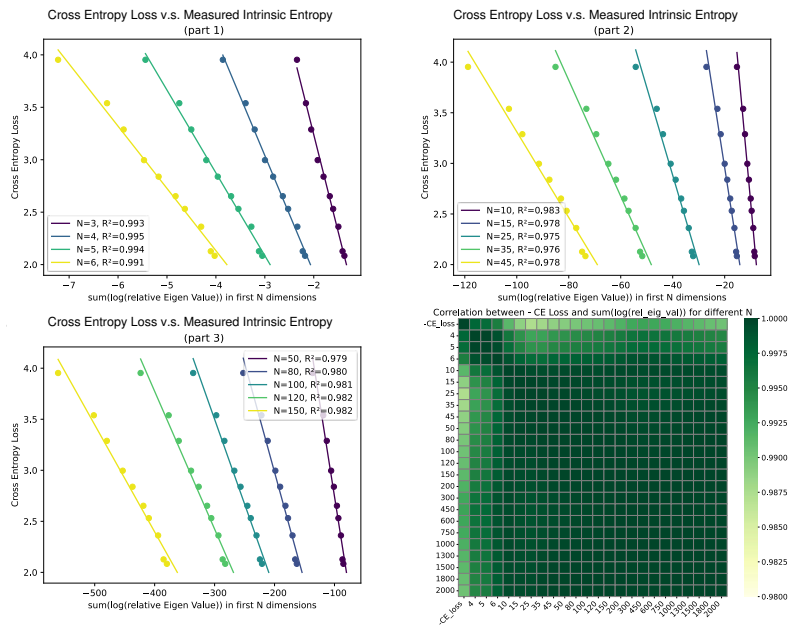


Figure 1: Upper-left, Upper-right, Bottom-left: **Cross Entropy Loss vs. measured Intrinsic Entropy** with  $N$  first Eigen Values:  $\sum_{i \leq N} \log \text{rel\_eig\_val}$ ; Bottom-right: correlation between minus CE loss and  $\sum_{i \leq N} \log \text{rel\_eig\_val}$ . All experiments are for LLaMa-3.1-8B on a subset of OpenWebText. From the first three figure, we see CE loss is linear with the Entropy of certain subspaces. From the bottom-right figure, we see that Entropy measured in different subspaces are highly correlated ( $\text{corr} > 0.97$ ), which are also highly correlated with the CE loss for Next Token Prediction. [More details about experiment settings can be found in Section 2.2.2.](#)

- 2. We conduct experiments on real and synthetic data, validating our theoretical assumptions and deductions.

The theoretical framework upon Intrinsic Entropy (with **formal definitions** in **Appendix D**) can predict or explain certain phenomena. For example, it shows that for a certain amount of training data, as the context length increases, the neural network would first behave more similarly to the Bayes model (thus the loss decreases); while beyond a certain optimal context length, the gap between the trained model and Bayes Model would increase, hence validation loss would increase: this is experimentally verified in Figure 4 of this work, and also related to certain observations in previous work.

We hope our work may inspire future work when it comes to explaining context impact and/or designing new long context Language Models.

## 2 ASSUMPTIONS, DEDUCTIONS AND OBSERVATIONS FOR LANGUAGE MODELING

### 2.1 PRELIMINARIES

#### 2.1.1 PRELIMINARY: LOSS DECOMPOSITION

It is common in ML studies to decompose the loss into **Bayes Risk** (the minimum loss possible, achieved by the theoretically optimal Bayesian Model), and **Approximation Loss** (the loss measuring the ability of a trained model actually to approximate the Bayesian Model). Specifically for Cross-Entropy loss  $H$ , we have (please refer to **Appendix B.1** for **formal definitions** and **deriva-**

108 **tion details):**

$$\begin{aligned} H(P, Q_l) &= R_{Bayes} + L_{Approx} \\ &= H(P, P_l) + D_{KL}(P_l, Q_l) \end{aligned} \tag{1}$$

112 Where  $P = p(x_0|x_{-\infty:0})$  is the distribution of Natural Language (or our experimented dataset),  
 113  $P_l = p(x_0|x_{-l:0})$  is the Bayesian Model for context length  $l$  and  $Q_l = q(x_0|x_{-l:0})$  is the  
 114 learned Language Model of context length  $l$ .  $R_{Bayes} = H(P, P_l)$  is the **Bayes Risk** of opti-  
 115 mal model (the assumed ‘limit’ when we have infinite data points and model parameters) and  
 116  $L_{Approx} = D_{KL}(P_l, Q_l)$  is the **Approximation Loss**, which can be affected by dataset size  $D$ ,  
 117 etc. The Bayes Risk is model or data agnostic, only related to natural language itself and is limited  
 118 only by visible context length.

## 119 2.1.2 PRELIMINARY: INTRINSIC SPACE

121 In previous work (Bahri et al., 2024; Cheng et al., 2023), as a common practice, the ‘Data Manifold’  
 122 is often **defined** as the middle feature representation of well-trained neural networks, and **assump-**  
 123 **tions** are made on this kind of mid-representation, with experiments to **validate** these assumptions.  
 124 (Intrinsic Space is defined as the space where the Data Manifold lies.) We follow such practice in  
 125 main paper for clarity.

126 Meanwhile, the Data Manifold can be more formally defined by a mapping from input data to some  
 127 Intrinsic Space which satisfies a certain set of properties, and mid-representation of well-trained  
 128 neural networks are assumed to have such properties, which can be experimentally validated. This  
 129 is an equivalent yet more formal perspective. In Appendix D, we formally define the Intrinsic Space  
 130 and derive related results in our work with such perspective for completeness.

## 132 2.1.3 PRELIMINARY: OUTLINES

133 In **Section 2.2** we propose the definition of Intrinsic Entropy, and discuss how to bridge **Bayes Risk**  
 134 with it, thus explaining how context length impacts Bayes Risk.

136 Approximation Loss, or how well the trained model learns Bayesian Model, is related to Intrinsic  
 137 Dimension in previous work of Scaling Laws (Sharma & Kaplan, 2022; Shi et al., 2024). In  
 138 **Section 2.3** we discuss more about how the context length impacts **Approximation Loss** from this  
 139 perspective.

140 We further derive that the balance between **Bayes Risk** and **Approximation Loss** would lead to  
 141 an optimal context length which increases with the size of the training dataset. Our theoretical  
 142 deduction and experiments on language are presented in **Section 3**.

## 144 2.2 BAYES RISK WITH CONTEXT LENGTH: AN INTRINSIC ENTROPY PERSPECTIVE

145 In this section we discuss to bridge context length and Bayes Risk with the concept of Intrinsic  
 146 Entropy.

## 148 2.2.1 BAYES RISK AND ENTROPY IN INTRINSIC SPACE: DERIVED FROM FIRST PRINCIPLES

150 ‘Information Entropy’ is defined as the amount of information carried in the Intrinsic Space. Here  
 151 are detailed assumptions<sup>4</sup> as definitions:<sup>5</sup>

- 153 • **Assumption 1.** Information Entropy of Intrinsic Space for Bayes Model  $\lim_{l \rightarrow \infty} S(P_l) = S(P_\infty)$  is finite, which is the Information Entropy of next token prediction of language  
 154 itself.
- 156 • **Assumption 2.**  $\forall l_1, l_2$  such that  $l_1 < l_2$ ,  $S(P_{l_1}) < S(P_{l_2})$ . This is because a longer  
 157 context contains more information.
- 158 • **Assumption 3. Linear Entropy Relationship:** The Information Entropy w.r.t. Next Token  
 159 Prediction, defined as  $S_{ntp}(P_l) = H(P_0) - H(P_l)$ , is linear with the Entropy in the Intrinsic

161 <sup>4</sup>Appendix D defines Intrinsic Entropy from a more formal perspective.

<sup>5</sup>To avoid confusion, we use ‘H’ for ‘Cross Entropy Loss’, and ‘S’ for ‘Information Entropy’.

162 Space of the Bayes Model, i.e.,  $S_{ntp}(P_l) = k * S(P_l) + b$ , and  $0 < k < 1$ . A **formal**  
 163 **definition can be found in Appendix D.**

164  $S_{ntp}$  is smaller than  $S$  since the Intrinsic Space contains important information on previous  
 165 tokens that are important for the prediction of future tokens, while  $S_{ntp}$  is related only to the  
 166 next token. The hidden state in RNNs contain more information than only the next token  
 167 to predict. For example, consider a character-level RNN that predicts the sentence ‘1 + 2  
 168 equal\_’, the next character to predict is ‘s’, but the hidden state should contain information  
 169 about answer ‘3’ for the latter tokens.

170 With these assumptions, we can derive that the Bayes Risk is linear with respect to the Intrinsic  
 171 Entropy:  
 172

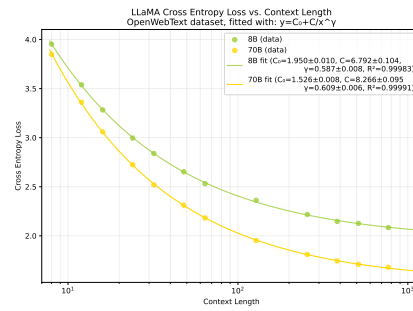
$$173 \quad R_{Bayes} = H(P, P_l) \\ 174 \quad = -k * S(P_l) + Const \quad (2)$$

175 This **linear relationship** is observed in experiments for LMs in **Section 2.2.2**, and for synthetic data  
 176 in **Section 4.3**.

177 Note that by Assumptions 1 and 2 we derive: <sup>6</sup>  $\frac{\partial R_{Bayes}}{\partial l} < 0$ , and  $\lim_{l \rightarrow \infty} \frac{\partial R_{Bayes}}{\partial l} = 0$ .

### 178 2.2.2 BAYES RISK AND INTRINSIC ENTROPY: EXPERIMENT MEASUREMENT

179 We use well-trained Large Language Models to conduct experiments for approximating the Bayes  
 180 Risk  $H(P_l)$  on certain text corpora.



181 Figure 2: **Bayes Risk vs. Context Length**: Bayes Risk is approximated by Cross Entropy loss  
 182 measured with LLaMa-3.1 series on OpenWebText, for different context length.

183 We find that:

$$184 \quad H(P, P_l) \approx C_0 + C/l^\gamma \quad (3)$$

185 approximates the experimented behavior on OpenWebText well. Please see Figure 2 for the result.  
 186 Moreover, we further conduct experiments on a dataset that is sure not to be included in LLaMa  
 187 3.1 8B’s pretraining dataset. Please see further information in Appendix E.

188 **Experimentally measure Intrinsic Entropy  $S$  using Eigen Values as proxy** To establish a relation-  
 189 ship between Cross Entropy and Intrinsic Space, we run LLaMa-3-8b on a subset of the Open-  
 190 webtext dataset and obtain the feature of the last token as the feature representation, or Intrinsic  
 191 Space of the approximated Bayes Model. **For certain context length, we gather the feature repre-  
 192 sentation of multiple ( $\geq 10000$ ) samples, and conduct PCA analysis on these samples to obtain**

193 <sup>6</sup>Generally speaking, the context length  $l$  is an integer. Here, following previous work (Kaplan et al.,  
 194 2020; Tao et al., 2024), we assume  $R_{Bayes}$  admits a differentiable extension  $\tilde{R}_{Bayes}$  to real-valued  $l$  and use  
 195  $\partial R_{Bayes}/\partial l$  to denote  $\partial \tilde{R}_{Bayes}(l)/\partial l$  evaluated at integer  $l$ . In this sense, the derivative serves as a continuous  
 196 approximation to the discrete difference  $R_{Bayes}(l+1) - R_{Bayes}(l)$ . We use the same convention for expressions  
 197 of the form  $df(l)/dl$  throughout this work.

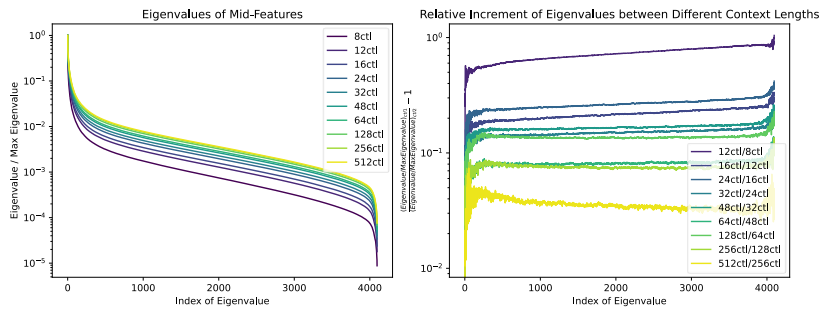
216  
217  
218  
219  
220  
221  
222  
223  
224  
225  
226  
227

Figure 3: **Left:** **Relative Eigen Value** Measured for the last token, for LLaMa-3.1-8B on a subset of OpenWebText. **Right:** relative increment of relative eigenvalues (for different context lengths measured). We can see that the relative eigenvalues approximately increase at a same scale.

231

eigenvalues for the specific context length, results are presented in Figure 1. We see that the model with larger context length tends to have larger relative eigenvalues in intrinsic space, thus containing more information.

235  
236  
237

According to Statistical Physics, entropy of a system can be defined as  $S = \log \Omega$  where  $\Omega$  is the possible number of states of the system (Landau & Lifshitz, 1980). Similarly, we use the sum of logarithm of eigen values as proxy for measuring Information Entropy:<sup>7</sup>

238  
239  
240  
241  
242  
243  
244  
245

$$\begin{aligned} S &= \log \Omega \\ &= \log V/h^{\dim(V)} \text{ where } V \text{ is the volume in intrinsic space} \\ &= \sum_i \log \text{rel\_eigval}_i/h \\ &= \sum_i \log \text{rel\_eigval}_i + \text{Const} \end{aligned}$$

246  
247  
248  
249

Here  $h$  is the ‘plank constant’, meaning that one state corresponds to a unit hyper-volume of  $h^{\dim}$  in the Intrinsic Space. A different value of  $h$  would only add a constant to  $S$  and would not affect change in Entropy. Thus, we use  $\sum_i \log \text{rel\_eigval}_i$  as Entropy in Intrinsic Space.

250  
251  
252  
253  
254  
255  
256

**Experimentally measure next-token-prediction Information Entropy  $S_{ntp}$**  Experiments show that, no matter what subspace we use, the Cross Entropy Loss usually follows a linear relationship with the Entropy we measured in the subspace, supporting the claim that the next token prediction task likely lies in some subspace of the Intrinsic Space, or (statistically) its Entropy should be some weighted average of Entropy of several subspaces of similar dimension.. This also suggests that  $H_{ntp}$  is approximately linear with  $H_{IS}$ , which validates our previous assumptions and claims.

257  
258  
259

We observe a fairly linear relationship between CE Loss and Entropy measured (supporting our theory), validating our theoretical assumptions:

260

$$R_{Bayes} \approx -k * S(P_l) + \text{Const},$$

261  
262  
263

which aligns well with **Equation 2**, thus validating our entropy-based deduction.

264  
265

### 2.3 APPROXIMATION LOSS WITH CONTEXT LENGTH: AN INTRINSIC DIMENSION PERSPECTIVE

266  
267  
268  
269

Previous work experimentally summarizes the Scaling Laws (Kaplan et al., 2020; Hoffmann et al., 2022) as:  $L_{Approx}(D) = C_0 + A/D^\alpha$  for different dataset size  $D$ . Previous work has succeeded

<sup>7</sup>Similar estimation can also be derived from the assumption of Gaussian differential entropy with homogeneous reference measure.

270 in explaining this from an intrinsic space perspective, represented by (Bahri et al., 2024; Sharma &  
 271 Kaplan, 2022) as:  $\alpha \approx c/dim$ , and  $dim$  is the dimension of the data manifold of the data and the  
 272 model, where a uniform distribution in Intrinsic Space is assumed. **We derive this rigorously from  
 273 weaker assumptions in Theorem 1,2 in Appendix D.2.**

274 As assumed in Section 2.2.1, the Intrinsic Dimension should increase with  $l$ . Combined with previous  
 275 results on  $\alpha = c/dim(l)$ , we have,  
 276

$$277 \quad L_{Approx} = C_0 + A(l)/D^{\alpha(l)}, \\ 278 \quad \frac{\partial \alpha}{\partial l} < 0. \quad (4)$$

281 This shows longer context length would make it harder for the model to learn to approximate the  
 282 Bayes Model.  
 283

### 284 3 DEDUCTION: OPTIMAL CONTEXT LENGTH AND TRAINING DATASET SIZE

287 In this section, we show a deduction of our theory presented in Section 2. We study the problem  
 288 about a certain model trained on certain amount of training dataset  $D$  with context length  $l$ , and  
 289 validated on the validation set with the same context length  $l$ , where we want to know the impact of  
 290  $l$  on validation loss.

291 As shown in Section 2.2, we can write Loss as:

$$292 \quad H(P, Q_l) = C_0 + \frac{C}{l^\gamma} + \frac{A(l)}{D^{\alpha(l)}}, \quad (5)$$

295 In previous sections, we did not specifically discuss the relationship between  $A$  and  $l$ . We consider  
 296  $l$  where  $\partial_l L_{CE} = 0$  would give us an optimal  $l$  with respect to  $D$ :

$$297 \quad \partial_l A = -A \ln D(-\partial_l \alpha) + \gamma C \frac{D^\alpha}{l^{\gamma+1}} = f(D, l). \quad (6)$$

300 As shown,  $\lim_{D \rightarrow 0} f = -\infty$  and  $\lim_{D \rightarrow \infty} f = \infty$ . This shows that for fixed  $l$ , no matter what  $\partial_l A$   
 301 is, there exists some  $D$  s.t.  $\partial_l L_{CE} = 0$ .

303 Bayes Risk decreases with  $l$ , while Approximation Loss increases with  $l$  but decreases with  $D$ ; the  
 304 balance between these two losses results in an optimal  $l$  that increases with the optimal  $D$ .

305 We conduct experiments on a subset of OpenWebText with a sufficiently long context length. We  
 306 trained GPT-2 on different context lengths with different amounts of training data, until the valida-  
 307 tion loss increases. We show our results in **Figure 4** and **Figure 14**. Details for our experiment  
 308 settings are presented in the Appendix H.

309 As shown both theoretically and experimentally, there does exist an optimal context length, **beyond  
 310 which even relevant long context would increase validation loss** of pretraining Language Models.  
 311 Such optimal context length would increase with training dataset size.  
 312

## 313 4 PROOF OF CONCEPT WITH SYNTHETIC DATA

### 314 4.1 LIST OF POINTS TO PROVE

317 In this section, we conduct experiments on a synthetic dataset, explaining the Bayes Risk and re-  
 318 lated theories we proposed in Section 2.2. With this synthetic dataset, we would like to prove the  
 319 following,  
 320

- 321 • **Point 1. Cross Entropy** Loss is approximately linear with **Intrinsic Entropy** (Assumption 3 in  
 322 Section 2.2.1). Shown in **Section 4.3**.
- 323 • **Point 2.** By measuring **Entropy** in **Intrinsic Space** of well-trained models, one could obtain a **valid  
 324 measurement that is linear with Cross Entropy Loss** (Section 2.2.2). Shown in **Section 4.4**.

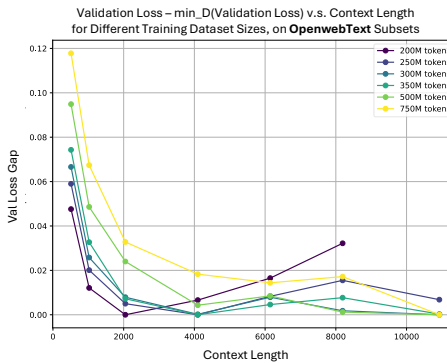


Figure 4: Validation Loss Gap (Val Loss -  $\min_D(\text{Val Loss})$ ) v.s. Context Length, measured on subsets of OpenWebText dataset, where we subtract the minimum loss grouped by context length from each curve (please refer to Figure 14 for the original figure). For each training dataset size, there exists an optimal context length that minimizes pretraining validation loss, which increases with the dataset size (More details can be found in [Section 3](#)). [We also provide similar experiments to prove an optimal context length exists on a synthetic dataset, as shown in Appendix F.](#)

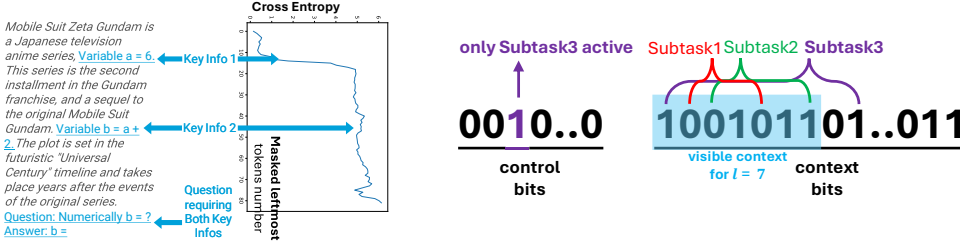


Figure 5: **Left:** An example of the ‘two needles in a haystack’ task, similar to those in (Levy et al., 2024). The text part is the input to the Language Model, with key information and question visualized in blue; the figure part shows perplexity of the answer token (8) of LLaMa-3.1-8B (horizontal) vs. number of masked leftmost tokens (vertical). Although seeing both pieces of information are necessary to answer the question, perplexity rises dramatically only when the first piece of information is masked. **Right:** An example of our synthetic data. [Each sub-task corresponds to 2 context bits of fixed position. At each time, exactly one sub-task is active, and the ground truth output is calculated by taking XOR over the 2 context bits of the activate task.](#) As shown in the example, the answer for Subtask 1,2,3 is  $0 \oplus 0 = 0$ ,  $0 \oplus 1 = 1$  and  $1 \oplus 1 = 0$  respectively, but since the third bit is 1 for control bits, only Subtask 3 is activated and the final answer is 0. However, for a model of context length 7, it cannot see the 9th bit required by subtask 3, making it unable to predict the answer correctly.

## 4.2 CONSTRUCTION OF SYNTHETIC DATA: THE ‘POSITION WEIGHTED MULTITASK SPARSE PARITY’ DATASET

In previous work, a common practice is to mask the leftmost tokens and leave  $l$  tokens before the token-to-predict visible to Language Models, as shown in Figure 5. Although this may not show the impact of important tokens to final answer perplexity (e.g., it fails to show the importance of the second key info in Figure 5), this method aligns well with our setting of increasing context length.

Although the next token to predict might depend on several pieces of key information, we see from Figure 5 that the first key token would raise model perplexity.

Inspired by this concept in Figure 5 and the ‘multitask sparse parity dataset previously studied in (Michaud et al., 2024; Barak et al., 2022), we propose the ‘position-weighted multitask sparse parity dataset. In detail, each input consists of  $L$  ‘context bits, each bit lies in  $\{0, 1\}$ . Each subtask takes

378 xor on two certain bits in the context bits, and the answer to some sample is the answer of the  
 379 only activated subtask, as shown in Figure 5. We use 60 context bits and 200 tasks. From 11th to  
 380 the 60th bit, each bit corresponds to the max bit of two tasks:  $\#Task|_{max(bit_1,bit_2)=i} = 2, \forall i \in$   
 381  $\{11, 12, \dots, 60\}$ .

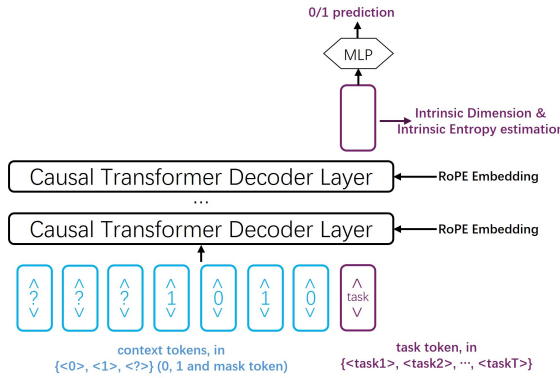
382 We assign different frequencies to different tasks, approximating the real-world situation where tasks  
 383 requiring nearer bits are more often. In all, Bayes Risk, or the minimum Cross Entropy Loss, is:  
 384

$$\begin{aligned}
 385 \quad & R_{Bayes}(ctl) \\
 386 \quad & = \text{MinCELoss}(ctl) \\
 387 \quad & = \left( \sum_{\substack{\text{task s.t.} \\ \text{max}(bit_1,bit_2) > ctl}} \text{freq(task)} \log 2 \right) / \sum_{\text{task}} \text{freq(task)} \\
 388 \quad & \approx A + B / (ctl + C)^\alpha
 \end{aligned}$$

392 More details are shown in Table 1.  
 393

### 394 4.3 TRANSFORMER-BASED SYNTHETIC MODEL WITH ENTROPY MEASUREMENTS

396 We use a 3-layer causal Transformer, with embedding dimension 208 and FFN dimension 832, RoPE  
 397 embedding with base frequency 4000; input sequence length is always 60+1, with 60 context tokens  
 398 (either 0, 1 or ?) and 1 task tokens (chosen from task tokens of vocab size 200).  
 399



413 Figure 6: Transformer and Rope-based model for the synthetic task. Here, we use one task token to  
 414 encode the task information.  
 415

416 We use 100 tasks and 60 task bits. From 11th to the 60th bit, each bit corresponds to the max bit of  
 417 two tasks: that is,  $\#Task|_{max(bit_1,bit_2)=i} = 2, \forall i \in \{11, 12, \dots, 60\}$ .  
 418

419 During training, 50% of the samples are unmasked, while for the other 50% samples, we mask the  
 420 last  $X$  task bits to be 0.5, where  $X$  is a random int from 60 – 10 to 60 – 60. This ensures our model  
 421 to be able to handle mask bits, and also ensures it can learn uncommon tasks (relying on context bits  
 422 that are at the end of the context bits) well. We train the model on large enough dataset so that it  
 423 approximates the Bayes Model well (please refer to Table 1 in Appendix for more details).

424 After the model has been trained, we measure its eigen values, as shown in Figure 7. It is shown that:  
 425 (1) Larger context length contains more information, hence eigen values in Intrinsic Space degrades  
 426 slower (left figure); (2) the model approximates the theoretical Bayes Model well (as the green  
 427 points in the middle figure is very close to the orange ones) (middle figure); (3) CE Loss follows a  
 428 very good linear relationship with sum of log eigenvalues of the first  $N$  dimensions for  $N \geq 70$  in  
 429 the Intrinsic Space (right figure), where the case  $N = 200$  (all eigen values) are also shown in the  
 430 middle figure.

431 This validates **Point 1**: Cross Entropy Loss is approximately linear with Intrinsic Entropy as mea-  
 432 sured by the sum of log eigenvalues.

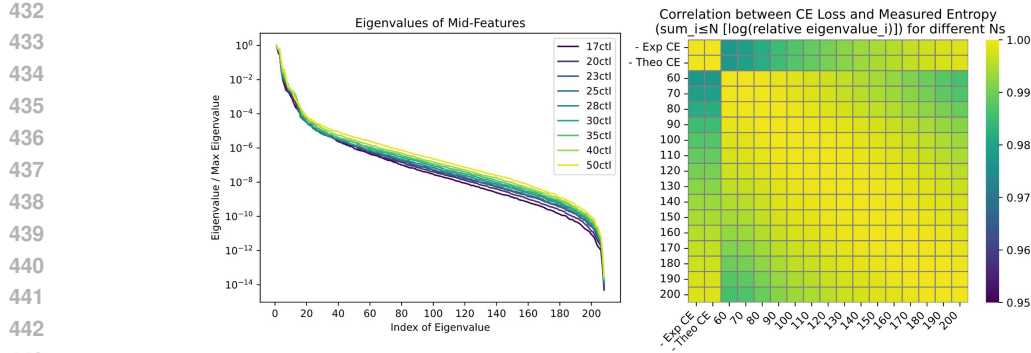


Figure 7: Eigen value and CE results measured on trained model for Synthetic Dataset in this section. **Left:** Eigen Value v.s. Index of Eigen Value; **Right:** Correlation between Cross Entropy Loss and Measured Entropy. We see good linear relationship between CE Losses and Measured Intrinsic Entropy from Lower figures.

#### 4.4 ENTROPY IN INTRINSIC SPACE: SYNTHETIC DATASET VALIDATION

Figure 7 shows the measured results of Intrinsic Entropy on the synthetic dataset, which follows a linear relationship with the Cross Entropy Calculated (Theo CE) and Cross Entropy loss measured (Exp CE).

This provides evidence for **Point 2** in Section 4.1: we can measure entropy in the intrinsic space using eigenvalue-based methods or density-based methods, and both show linear relationships with Cross Entropy Loss, validating our entropy-based theoretical framework.

## 5 CONCLUSION AND DISCUSSIONS

### 5.1 CONCLUSION

In this work, we discuss the impact of context length on language modeling, especially Bayes risk and approximate loss, from both a theoretical and experimental perspective.

In Section 2, we propose assumptions related to the relationship between **CE Loss**, **intrinsic entropy** and **context length**. We derive a linear relation between CE loss and Intrinsic Entropy, and study the impact of context length to intrinsic entropy. We further investigate the relationship between intrinsic entropy, context length, and Intrinsic Dimension in **Appendix J** from an **Intrinsic Dimension perspective**. We provide **formal definitions of assumptions and derivations of important theorems** in **Appendix D**.

We also conduct experiments with real data (Section 2, Section 3) and synthetic data (Section 4), on measuring Intrinsic Entropy and on the relationship between Cross Entropy Loss (Bayes Risk and Approximation Loss), Context Length and Intrinsic Entropy.

As a correlation of our theory, there exists an optimal context length that increases with dataset size in pretraining process. This is validated in Section 3. [For downstream task such as document QA for long documents, we conduct experiment and also observe an optimal context length which increases with tasks' typical context length for a certain model. This is shown in Appendix A.](#) We hope our work may provide insight for future work about long context Language Models, or about Physics for Language Models.

### 5.2 LIMITATIONS AND FUTURE WORK

Our theory starting from Intrinsic Entropy only holds with assumptions in Section 2; and in Appendix J we use the perspective of Intrinsic Dimension to (partially) explain our assumptions and measurements w.r.t. Intrinsic Entropy. We hope future work may try to propose even more fundamental theories to explain our Intrinsic Entropy measurements.

In our work, similar to several previous work (Bahri et al., 2024; Aghajanyan et al., 2021), we explain the impact of context length scaling from the perspective of Intrinsic Space (or Data Manifold), which is related not only to data, but also potentially to the neural network (that maps the data into such Intrinsic Space) and the prediction task (Bahri et al., 2024). Our explanation leans toward how the model represents the data in its intrinsic space and is hence more related to real language models, meanwhile other types of more model-agnostic explanations might also be proposed.

## REFERENCES

Armen Aghajanyan, Luke Zettlemoyer, and Sonal Gupta. Intrinsic dimensionality explains the effectiveness of language model fine-tuning, 2020. URL <https://arxiv.org/abs/2012.13255>.

Armen Aghajanyan, Sonal Gupta, and Luke Zettlemoyer. Intrinsic dimensionality explains the effectiveness of language model fine-tuning. In Chengqing Zong, Fei Xia, Wenjie Li, and Roberto Navigli (eds.), *Proceedings of the 59th Annual Meeting of the Association for Computational Linguistics and the 11th International Joint Conference on Natural Language Processing (Volume 1: Long Papers)*, pp. 7319–7328, Online, August 2021. Association for Computational Linguistics. doi: 10.18653/v1/2021.acl-long.568. URL <https://aclanthology.org/2021.acl-long.568/>.

Yasaman Bahri, Ethan Dyer, Jared Kaplan, Jaehoon Lee, and Utkarsh Sharma. Explaining neural scaling laws. *Proceedings of the National Academy of Sciences*, 121(27), June 2024. ISSN 1091-6490. doi: 10.1073/pnas.2311878121. URL <http://dx.doi.org/10.1073/pnas.2311878121>.

Boaz Barak, Benjamin L. Edelman, Surbhi Goel, Sham M. Kakade, eran malach, and Cyril Zhang. Hidden progress in deep learning: SGD learns parities near the computational limit. In Alice H. Oh, Alekh Agarwal, Danielle Belgrave, and Kyunghyun Cho (eds.), *Advances in Neural Information Processing Systems*, 2022. URL <https://openreview.net/forum?id=8XWP2ewX-im>.

Emily Cheng, Corentin Kervadec, and Marco Baroni. Bridging information-theoretic and geometric compression in language models. In Houda Bouamor, Juan Pino, and Kalika Bali (eds.), *Proceedings of the 2023 Conference on Empirical Methods in Natural Language Processing*, pp. 12397–12420, Singapore, December 2023. Association for Computational Linguistics. doi: 10.18653/v1/2023.emnlp-main.762. URL <https://aclanthology.org/2023.emnlp-main.762/>.

DeepSeek-AI, Aixin Liu, Bei Feng, Bing Xue, Bingxuan Wang, Bochao Wu, Chengda Lu, Chenggang Zhao, Chengqi Deng, Chenyu Zhang, Chong Ruan, Damai Dai, Daya Guo, Dejian Yang, Deli Chen, Dongjie Ji, Erhang Li, Fangyun Lin, Fucong Dai, Fuli Luo, Guangbo Hao, Guanting Chen, Guowei Li, H. Zhang, Han Bao, Hanwei Xu, Haocheng Wang, Haowei Zhang, Honghui Ding, Huajian Xin, Huazuo Gao, Hui Li, Hui Qu, J. L. Cai, Jian Liang, Jianzhong Guo, Jiaqi Ni, Jiashi Li, Jiawei Wang, Jin Chen, Jingchang Chen, Jingyang Yuan, Junjie Qiu, Junlong Li, Junxiao Song, Kai Dong, Kai Hu, Kaige Gao, Kang Guan, Kexin Huang, Kuai Yu, Lean Wang, Lecong Zhang, Lei Xu, Leyi Xia, Liang Zhao, Litong Wang, Liyue Zhang, Meng Li, Miaojun Wang, Mingchuan Zhang, Minghua Zhang, Minghui Tang, Mingming Li, Ning Tian, Panpan Huang, Peiyi Wang, Peng Zhang, Qiancheng Wang, Qihao Zhu, Qinyu Chen, Qiushi Du, R. J. Chen, R. L. Jin, Ruiqi Ge, Ruisong Zhang, Ruizhe Pan, Runji Wang, Runxin Xu, Ruoyu Zhang, Ruyi Chen, S. S. Li, Shanghao Lu, Shangyan Zhou, Shanhuang Chen, Shaoqing Wu, Shengfeng Ye, Shengfeng Ye, Shirong Ma, Shiyu Wang, Shuang Zhou, Shuiping Yu, Shunfeng Zhou, Shuting Pan, T. Wang, Tao Yun, Tian Pei, Tianyu Sun, W. L. Xiao, Wangding Zeng, Wanjia Zhao, Wei An, Wen Liu, Wenfeng Liang, Wenjun Gao, Wenqin Yu, Wentao Zhang, X. Q. Li, Xiangyue Jin, Xianzu Wang, Xiao Bi, Xiaodong Liu, Xiaohan Wang, Xiaojin Shen, Xiaokang Chen, Xiaokang Zhang, Xiaosha Chen, Xiaotao Nie, Xiaowen Sun, Xiaoxiang Wang, Xin Cheng, Xin Liu, Xin Xie, Xingchao Liu, Xingkai Yu, Xinnan Song, Xinxia Shan, Xinyi Zhou, Xinyu Yang, Xinyuan Li, Xuecheng Su, Xuheng Lin, Y. K. Li, Y. Q. Wang, Y. X. Wei, Y. X. Zhu, Yang Zhang, Yanhong Xu, Yanhong Xu, Yanping Huang, Yao Li, Yao Zhao, Yaofeng Sun, Yaohui Li, Yaohui Wang, Yi Yu, Yi Zheng, Yichao Zhang, Yifan Shi, Yiliang Xiong, Ying He, Ying

540 Tang, Yishi Piao, Yisong Wang, Yixuan Tan, Yiyang Ma, Yiyuan Liu, Yongqiang Guo, Yu Wu,  
 541 Yuan Ou, Yuchen Zhu, Yuduan Wang, Yue Gong, Yuheng Zou, Yujia He, Yukun Zha, Yunfan  
 542 Xiong, Yunxian Ma, Yuting Yan, Yuxiang Luo, Yuxiang You, Yuxuan Liu, Yuyang Zhou, Z. F.  
 543 Wu, Z. Z. Ren, Zehui Ren, Zhangli Sha, Zhe Fu, Zhean Xu, Zhen Huang, Zhen Zhang, Zhenda  
 544 Xie, Zhengyan Zhang, Zhewen Hao, Zhibin Gou, Zhicheng Ma, Zhigang Yan, Zhihong Shao,  
 545 Zhipeng Xu, Zhiyu Wu, Zhongyu Zhang, Zhuoshu Li, Zihui Gu, Zijia Zhu, Zijun Liu, Zilin Li,  
 546 Ziwei Xie, Ziyang Song, Ziyi Gao, and Zizheng Pan. Deepseek-v3 technical report, 2024. URL  
 547 <https://arxiv.org/abs/2412.19437>.

548 Aaron Grattafiori, Abhimanyu Dubey, Abhinav Jauhri, Abhinav Pandey, Abhishek Kadian, Ahmad  
 549 Al-Dahle, Aiesha Letman, Akhil Mathur, Alan Schelten, Alex Vaughan, Amy Yang, Angela Fan,  
 550 Anirudh Goyal, Anthony Hartshorn, Aobo Yang, Archi Mitra, Archie Sravankumar, Artem Ko-  
 551 rennev, Arthur Hinsvark, Arun Rao, Aston Zhang, Aurelien Rodriguez, Austen Gregerson, Ava  
 552 Spataru, Baptiste Roziere, Bethany Biron, Binh Tang, Bobbie Chern, Charlotte Caucheteux,  
 553 Chaya Nayak, Chloe Bi, Chris Marra, Chris McConnell, Christian Keller, Christophe Touret,  
 554 Chunyang Wu, Corinne Wong, Cristian Canton Ferrer, Cyrus Nikolaidis, Damien Allonsius,  
 555 Daniel Song, Danielle Pintz, Danny Livshits, Danny Wyatt, David Esiobu, Dhruv Choudhary,  
 556 Dhruv Mahajan, Diego Garcia-Olano, Diego Perino, Dieuwke Hupkes, Egor Lakomkin, Ehab  
 557 AlBadawy, Elina Lobanova, Emily Dinan, Eric Michael Smith, Filip Radenovic, Francisco  
 558 Guzmán, Frank Zhang, Gabriel Synnaeve, Gabrielle Lee, Georgia Lewis Anderson, Govind That-  
 559 tai, Graeme Nail, Gregoire Mialon, Guan Pang, Guillem Cucurell, Hailey Nguyen, Hannah Kore-  
 560 vaar, Hu Xu, Hugo Touvron, Iliyan Zarov, Imanol Arrieta Ibarra, Isabel Kloumann, Ishan Misra,  
 561 Ivan Evtimov, Jack Zhang, Jade Copet, Jaewon Lee, Jan Geffert, Jana Vranes, Jason Park, Jay Ma-  
 562 hadeokar, Jeet Shah, Jelmer van der Linde, Jennifer Billock, Jenny Hong, Jenya Lee, Jeremy Fu,  
 563 Jianfeng Chi, Jianyu Huang, Jiawen Liu, Jie Wang, Jiecao Yu, Joanna Bitton, Joe Spisak, Jong-  
 564 so Park, Joseph Rocca, Joshua Johnstun, Joshua Saxe, Junteng Jia, Kalyan Vasuden Alwala,  
 565 Karthik Prasad, Kartikeya Upasani, Kate Plawiak, Ke Li, Kenneth Heafield, Kevin Stone, Khalid  
 566 El-Arini, Krithika Iyer, Kshitiz Malik, Kuenley Chiu, Kunal Bhalla, Kushal Lakhota, Lauren  
 567 Rantala-Yearly, Laurens van der Maaten, Lawrence Chen, Liang Tan, Liz Jenkins, Louis Martin,  
 568 Lovish Madaan, Lubo Malo, Lukas Blecher, Lukas Landzaat, Luke de Oliveira, Madeline Muzzi,  
 569 Mahesh Pasupuleti, Mannat Singh, Manohar Paluri, Marcin Kardas, Maria Tsimpoukelli, Mathew  
 570 Oldham, Mathieu Rita, Maya Pavlova, Melanie Kambadur, Mike Lewis, Min Si, Mitesh Ku-  
 571 mar Singh, Mona Hassan, Naman Goyal, Narjes Torabi, Nikolay Bashlykov, Nikolay Bogoy-  
 572 chev, Niladri Chatterji, Ning Zhang, Olivier Duchenne, Onur Çelebi, Patrick Alrassy, Pengchuan  
 573 Zhang, Pengwei Li, Petar Vasic, Peter Weng, Prajjwal Bhargava, Pratik Dubal, Praveen Krishnan,  
 574 Punit Singh Koura, Puxin Xu, Qing He, Qingxiao Dong, Ragavan Srinivasan, Raj Ganapathy, Ra-  
 575 mon Calderer, Ricardo Silveira Cabral, Robert Stojnic, Roberta Raileanu, Rohan Maheswari, Ro-  
 576 hit Girdhar, Rohit Patel, Romain Sauvestre, Ronnie Polidoro, Roshan Sumbaly, Ross Taylor, Ruan  
 577 Silva, Rui Hou, Rui Wang, Saghar Hosseini, Sahana Chennabasappa, Sanjay Singh, Sean Bell,  
 578 Seohyun Sonia Kim, Sergey Edunov, Shaoliang Nie, Sharan Narang, Sharath Raparthy, Sheng  
 579 Shen, Shengye Wan, Shruti Bhosale, Shun Zhang, Simon Vandenhende, Soumya Batra, Spencer  
 580 Whitman, Sten Sootla, Stephane Collot, Suchin Gururangan, Sydney Borodinsky, Tamar Herman,  
 581 Tara Fowler, Tarek Sheasha, Thomas Georgiou, Thomas Scialom, Tobias Speckbacher, Todor Mi-  
 582 haylov, Tong Xiao, Ujjwal Karn, Vedanuj Goswami, Vibhor Gupta, Vignesh Ramanathan, Viktor  
 583 Kerkez, Vincent Gonguet, Virginie Do, Vish Vogeti, Vítor Albiero, Vladan Petrovic, Weiwei  
 584 Chu, Wenhan Xiong, Wenyin Fu, Whitney Meers, Xavier Martinet, Xiaodong Wang, Xiaofang  
 585 Wang, Xiaoqing Ellen Tan, Xide Xia, Xinfeng Xie, Xuchao Jia, Xuewei Wang, Yaelle Gold-  
 586 schlag, Yashesh Gaur, Yasmine Babaei, Yi Wen, Yiwen Song, Yuchen Zhang, Yue Li, Yuning  
 587 Mao, Zacharie Delpierre Coudert, Zheng Yan, Zhengxing Chen, Zoe Papakipos, Aaditya Singh,  
 588 Aayushi Srivastava, Abha Jain, Adam Kelsey, Adam Shajnfeld, Adithya Gangidi, Adolfo Victoria,  
 589 Ahuva Goldstand, Ajay Menon, Ajay Sharma, Alex Boesenberg, Alexei Baevski, Allie Feinstein,  
 590 Amanda Kallet, Amit Sangani, Amos Teo, Anam Yunus, Andrei Lupu, Andres Alvarado, An-  
 591 drew Caples, Andrew Gu, Andrew Ho, Andrew Poulton, Andrew Ryan, Ankit Ramchandani, An-  
 592 nie Dong, Annie Franco, Anuj Goyal, Aparajita Saraf, Arkabandhu Chowdhury, Ashley Gabriel,  
 593 Ashwin Bharambe, Assaf Eisenman, Azadeh Yazdan, Beau James, Ben Maurer, Benjamin Leon-  
 hardi, Bernie Huang, Beth Loyd, Beto De Paola, Bhargavi Paranjape, Bing Liu, Bo Wu, Boyu  
 Ni, Braden Hancock, Bram Wasti, Brandon Spence, Brani Stojkovic, Brian Gamido, Britt Mont-  
 talvo, Carl Parker, Carly Burton, Catalina Mejia, Ce Liu, Changhan Wang, Changkyu Kim, Chao  
 Zhou, Chester Hu, Ching-Hsiang Chu, Chris Cai, Chris Tindal, Christoph Feichtenhofer, Cynthia

594 Gao, Damon Civin, Dana Beaty, Daniel Kreymer, Daniel Li, David Adkins, David Xu, Davide  
 595 Testuggine, Delia David, Devi Parikh, Diana Liskovich, Didem Foss, Dingkang Wang, Duc Le,  
 596 Dustin Holland, Edward Dowling, Eissa Jamil, Elaine Montgomery, Eleonora Presani, Emily  
 597 Hahn, Emily Wood, Eric-Tuan Le, Erik Brinkman, Esteban Arcaute, Evan Dunbar, Evan Smothers,  
 598 Fei Sun, Felix Kreuk, Feng Tian, Filippos Kokkinos, Firat Ozgenel, Francesco Caggioni,  
 599 Frank Kanayet, Frank Seide, Gabriela Medina Florez, Gabriella Schwarz, Gada Badeer, Georgia  
 600 Swee, Gil Halpern, Grant Herman, Grigory Sizov, Guangyi, Zhang, Guna Lakshminarayanan,  
 601 Hakan Inan, Hamid Shojanazeri, Han Zou, Hannah Wang, Hanwen Zha, Haroun Habeeb, Harri-  
 602 son Rudolph, Helen Suk, Henry Aspegen, Hunter Goldman, Hongyuan Zhan, Ibrahim Damlaj,  
 603 Igor Molybog, Igor Tufanov, Ilias Leontiadis, Irina-Elena Veliche, Itai Gat, Jake Weissman, James  
 604 Geboski, James Kohli, Janice Lam, Japhet Asher, Jean-Baptiste Gaya, Jeff Marcus, Jeff Tang, Jen-  
 605 nifer Chan, Jenny Zhen, Jeremy Reizenstein, Jeremy Teboul, Jessica Zhong, Jian Jin, Jingyi Yang,  
 606 Joe Cummings, Jon Carvill, Jon Shepard, Jonathan McPhie, Jonathan Torres, Josh Ginsburg, Jun-  
 607 jie Wang, Kai Wu, Kam Hou U, Karan Saxena, Kartikay Khandelwal, Katayoun Zand, Kathy  
 608 Matosich, Kaushik Veeraraghavan, Kelly Michelena, Keqian Li, Kiran Jagadeesh, Kun Huang,  
 609 Kunal Chawla, Kyle Huang, Lailin Chen, Lakshya Garg, Lavender A, Leandro Silva, Lee Bell,  
 610 Lei Zhang, Liangpeng Guo, Licheng Yu, Liron Moshkovich, Luca Wehrstedt, Madian Khabsa,  
 611 Manav Avalani, Manish Bhatt, Martynas Mankus, Matan Hasson, Matthew Lennie, Matthias  
 612 Reso, Maxim Groshev, Maxim Naumov, Maya Lathi, Meghan Keneally, Miao Liu, Michael L.  
 613 Seltzer, Michal Valko, Michelle Restrepo, Mihir Patel, Mik Vyatskov, Mikayel Samvelyan, Mike  
 614 Clark, Mike Macey, Mike Wang, Miquel Jubert Hermoso, Mo Metanat, Mohammad Rastegari,  
 615 Munish Bansal, Nandhini Santhanam, Natascha Parks, Natasha White, Navyata Bawa, Nayan  
 616 Singhal, Nick Egebo, Nicolas Usunier, Nikhil Mehta, Nikolay Pavlovich Laptev, Ning Dong,  
 617 Norman Cheng, Oleg Chernoguz, Olivia Hart, Omkar Salpekar, Ozlem Kalinli, Parkin Kent,  
 618 Parth Parekh, Paul Saab, Pavan Balaji, Pedro Rittner, Philip Bontrager, Pierre Roux, Piotr Dollar,  
 619 Polina Zvyagina, Prashant Ratanchandani, Pritish Yuvraj, Qian Liang, Rachad Alao, Rachel Ro-  
 620 driguez, Rafi Ayub, Raghatham Murthy, Raghu Nayani, Rahul Mitra, Rangaprabhu Parthasarathy,  
 621 Raymond Li, Rebekkah Hogan, Robin Battey, Rocky Wang, Russ Howes, Ruty Rinott, Sachin  
 622 Mehta, Sachin Siby, Sai Jayesh Bondu, Samyak Datta, Sara Chugh, Sara Hunt, Sargun Dhillon,  
 623 Sasha Sidorov, Satadru Pan, Saurabh Mahajan, Saurabh Verma, Seiji Yamamoto, Sharadh Ra-  
 624 maswamy, Shaun Lindsay, Shaun Lindsay, Sheng Feng, Shenghao Lin, Shengxin Cindy Zha,  
 625 Shishir Patil, Shiva Shankar, Shuqiang Zhang, Shuqiang Zhang, Sinong Wang, Sneha Agarwal,  
 626 Soji Sajuyigbe, Soumith Chintala, Stephanie Max, Stephen Chen, Steve Kehoe, Steve Satter-  
 627 field, Sudarshan Govindaprasad, Sumit Gupta, Summer Deng, Sungmin Cho, Sunny Virk, Suraj  
 628 Subramanian, Sy Choudhury, Sydney Goldman, Tal Remez, Tamar Glaser, Tamara Best, Thilo  
 629 Koehler, Thomas Robinson, Tianhe Li, Tianjun Zhang, Tim Matthews, Timothy Chou, Tzook  
 630 Shaked, Varun Vontimitta, Victoria Ajayi, Victoria Montanez, Vijai Mohan, Vinay Satish Ku-  
 631 mar, Vishal Mangla, Vlad Ionescu, Vlad Poenaru, Vlad Tiberiu Mihaiescu, Vladimir Ivanov,  
 632 Wei Li, Wencheng Wang, Wenwen Jiang, Wes Bouaziz, Will Constable, Xiaocheng Tang, Xiao-  
 633 jian Wu, Xiaolan Wang, Xilun Wu, Xinbo Gao, Yaniv Kleinman, Yanjun Chen, Ye Hu, Ye Jia,  
 634 Ye Qi, Yenda Li, Yilin Zhang, Ying Zhang, Yossi Adi, Youngjin Nam, Yu, Wang, Yu Zhao,  
 635 Yuchen Hao, Yundi Qian, Yunlu Li, Yuzi He, Zach Rait, Zachary DeVito, Zef Rosnbrick, Zhao-  
 636 duo Wen, Zhenyu Yang, Zhiwei Zhao, and Zhiyu Ma. The llama 3 herd of models, 2024. URL  
 637 <https://arxiv.org/abs/2407.21783>.

638 Albert Gu and Tri Dao. Mamba: Linear-time sequence modeling with selective state spaces, 2024.  
 639 URL <https://arxiv.org/abs/2312.00752>.

640 Alexander Havrilla and Wenjing Liao. Understanding scaling laws with statistical and approxima-  
 641 tion theory for transformer neural networks on intrinsically low-dimensional data. In *The Thirty-  
 642 eighth Annual Conference on Neural Information Processing Systems*, 2024. URL <https://openreview.net/forum?id=N2wYPMpifA>.

643 Jordan Hoffmann, Sebastian Borgeaud, Arthur Mensch, Elena Buchatskaya, Trevor Cai, Eliza  
 644 Rutherford, Diego de Las Casas, Lisa Anne Hendricks, Johannes Welbl, Aidan Clark, Tom Hen-  
 645 nigan, Eric Noland, Katie Millican, George van den Driessche, Bogdan Damoc, Aurelia Guy,  
 646 Simon Osindero, Karen Simonyan, Erich Elsen, Jack W. Rae, Oriol Vinyals, and Laurent Sifre.  
 647 Training compute-optimal large language models, 2022. URL <https://arxiv.org/abs/2203.15556>.

648 Cheng-Ping Hsieh, Simeng Sun, Samuel Kriman, Shantanu Acharya, Dima Rekesh, Fei Jia, and  
 649 Boris Ginsburg. RULER: What's the real context size of your long-context language models? In  
 650 *First Conference on Language Modeling*, 2024. URL <https://openreview.net/forum?id=kIoBbc76Sy>.

652 Jared Kaplan, Sam McCandlish, Tom Henighan, Tom B. Brown, Benjamin Chess, Rewon Child,  
 653 Scott Gray, Alec Radford, Jeffrey Wu, and Dario Amodei. Scaling laws for neural language  
 654 models, 2020. URL <https://arxiv.org/abs/2001.08361>.

656 Andrej Karpathy. NanoGPT. <https://github.com/karpathy/nanoGPT>, 2022.

657 Angelos Katharopoulos, Apoorv Vyas, Nikolaos Pappas, and François Fleuret. Transformers are  
 658 rnns: Fast autoregressive transformers with linear attention, 2020. URL <https://arxiv.org/abs/2006.16236>.

660 L.D. Landau and E.M. Lifshitz. *Statistical Physics*, volume 5 of *Course of Theoretical Physics*.  
 661 Butterworth-Heinemann, Oxford, 3 edition, 1980. ISBN 978-0-7506-3372-7.

663 Mosh Levy, Alon Jacoby, and Yoav Goldberg. Same task, more tokens: the impact of input length  
 664 on the reasoning performance of large language models, 2024. URL <https://arxiv.org/abs/2402.14848>.

666 Ilya Loshchilov and Frank Hutter. Decoupled weight decay regularization, 2019. URL <https://arxiv.org/abs/1711.05101>.

668 Eric J. Michaud, Ziming Liu, Uzay Girit, and Max Tegmark. The quantization model of neural  
 669 scaling, 2024. URL <https://arxiv.org/abs/2303.13506>.

671 Bo Peng, Eric Alcaide, Quentin Anthony, Alon Albalak, Samuel Arcadinho, Stella Biderman,  
 672 Huanqi Cao, Xin Cheng, Michael Chung, Matteo Grella, Kranthi Kiran GV, Xuzheng He, Haowen  
 673 Hou, Jiaju Lin, Przemyslaw Kazienko, Jan Kocon, Jiaming Kong, Bartłomiej Koptyra, Hayden  
 674 Lau, Krishna Sri Ipsit Mantri, Ferdinand Mom, Atsushi Saito, Guangyu Song, Xiangru Tang,  
 675 Bolun Wang, Johan S. Wind, Stanislaw Wozniak, Ruchong Zhang, Zhenyuan Zhang, Qihang  
 676 Zhao, Peng Zhou, Qinghua Zhou, Jian Zhu, and Rui-Jie Zhu. Rwkv: Reinventing rnns for the  
 677 transformer era, 2023. URL <https://arxiv.org/abs/2305.13048>.

678 Alec Radford, Jeff Wu, Rewon Child, David Luan, Dario Amodei, and Ilya Sutskever. Language  
 679 models are unsupervised multitask learners. 2019.

680 Colin Raffel, Noam Shazeer, Adam Roberts, Katherine Lee, Sharan Narang, Michael Matena, Yanqi  
 681 Zhou, Wei Li, and Peter J. Liu. Exploring the limits of transfer learning with a unified text-to-text  
 682 transformer, 2023. URL <https://arxiv.org/abs/1910.10683>.

684 Pranav Rajpurkar, Jian Zhang, Konstantin Lopyrev, and Percy Liang. Squad: 100,000+ questions  
 685 for machine comprehension of text, 2016. URL <https://arxiv.org/abs/1606.05250>.

686 Utkarsh Sharma and Jared Kaplan. A neural scaling law from the dimension of the data manifold,  
 687 2020. URL <https://arxiv.org/abs/2004.10802>.

689 Utkarsh Sharma and Jared Kaplan. Scaling laws from the data manifold dimension. *Journal of  
 690 Machine Learning Research*, 23(9):1–34, 2022. URL <http://jmlr.org/papers/v23/20-1111.html>.

692 Jingzhe Shi, Qinwei Ma, Huan Ma, and Lei Li. Scaling law for time series forecasting. In *The Thirty-  
 693 eighth Annual Conference on Neural Information Processing Systems*, 2024. URL <https://openreview.net/forum?id=Cr2jEHJB9q>.

695 Jianlin Su, Yu Lu, Shengfeng Pan, Ahmed Murtadha, Bo Wen, and Yunfeng Liu. Roformer: En-  
 696 hanced transformer with rotary position embedding, 2023. URL <https://arxiv.org/abs/2104.09864>.

698 Yu Sun, Xinhao Li, Karan Dalal, Jiarui Xu, Arjun Vikram, Genghan Zhang, Yann Dubois, Xinlei  
 699 Chen, Xiaolong Wang, Sanmi Koyejo, Tatsunori Hashimoto, and Carlos Guestrin. Learning to  
 700 (learn at test time): Rnns with expressive hidden states, 2024. URL <https://arxiv.org/abs/2407.04620>.

702 Hanlin Tang, Yang Lin, Jing Lin, Qingsen Han, Shikuan Hong, Yiwu Yao, and Gongyi Wang.  
 703 Razorattention: Efficient kv cache compression through retrieval heads, 2024. URL <https://arxiv.org/abs/2407.15891>.  
 704

705 Chaofan Tao, Qian Liu, Longxu Dou, Niklas Muennighoff, Zhongwei Wan, Ping Luo, Min Lin,  
 706 and Ngai Wong. Scaling laws with vocabulary: Larger models deserve larger vocabularies, 2024.  
 707 URL <https://arxiv.org/abs/2407.13623>.  
 708

709 Wenzheng Xiong, Jingyu Liu, Igor Molybog, Hejia Zhang, Prajjwal Bhargava, Rui Hou, Louis Mar-  
 710 tin, Rashi Rungta, Karthik Abinav Sankararaman, Barlas Oguz, Madiyan Khabsa, Han Fang,  
 711 Yashar Mehdad, Sharan Narang, Kshitiz Malik, Angela Fan, Shruti Bhosale, Sergey Edunov,  
 712 Mike Lewis, Sinong Wang, and Hao Ma. Effective long-context scaling of foundation mod-  
 713 els. In Kevin Duh, Helena Gomez, and Steven Bethard (eds.), *Proceedings of the 2024 Confer-  
 714 ence of the North American Chapter of the Association for Computational Linguistics: Human  
 715 Language Technologies (Volume 1: Long Papers)*, pp. 4643–4663, Mexico City, Mexico, June  
 716 2024. Association for Computational Linguistics. doi: 10.18653/v1/2024.naacl-long.260. URL  
 717 <https://aclanthology.org/2024.naacl-long.260>.  
 718

718 Peng Xu, Wei Ping, Xianchao Wu, Lawrence McAfee, Chen Zhu, Zihan Liu, Sandeep Subramanian,  
 719 Evelina Bakhturina, Mohammad Shoeybi, and Bryan Catanzaro. Retrieval meets long context  
 720 large language models, 2024. URL <https://arxiv.org/abs/2310.03025>.  
 721

722 An Yang, Anfeng Li, Baosong Yang, Beichen Zhang, Binyuan Hui, Bo Zheng, Bowen Yu, Chang  
 723 Gao, Chengan Huang, Chenxu Lv, Chujie Zheng, Dayiheng Liu, Fan Zhou, Fei Huang, Feng Hu,  
 724 Hao Ge, Haoran Wei, Huan Lin, Jialong Tang, Jian Yang, Jianhong Tu, Jianwei Zhang, Jianxin  
 725 Yang, Jiaxi Yang, Jing Zhou, Jingren Zhou, Junyang Lin, Kai Dang, Keqin Bao, Kexin Yang,  
 726 Le Yu, Lianghao Deng, Mei Li, Mingfeng Xue, Mingze Li, Pei Zhang, Peng Wang, Qin Zhu, Rui  
 727 Men, Ruize Gao, Shixuan Liu, Shuang Luo, Tianhao Li, Tianyi Tang, Wenbiao Yin, Xingzhang  
 728 Ren, Xinyu Wang, Xinyu Zhang, Xuancheng Ren, Yang Fan, Yang Su, Yichang Zhang, Yinger  
 729 Zhang, Yu Wan, Yuqiong Liu, Zekun Wang, Zeyu Cui, Zhenru Zhang, Zhipeng Zhou, and Zihan  
 730 Qiu. Qwen3 technical report, 2025. URL <https://arxiv.org/abs/2505.09388>.  
 731  
 732  
 733  
 734  
 735  
 736  
 737  
 738  
 739  
 740  
 741  
 742  
 743  
 744  
 745  
 746  
 747  
 748  
 749  
 750  
 751  
 752  
 753  
 754  
 755

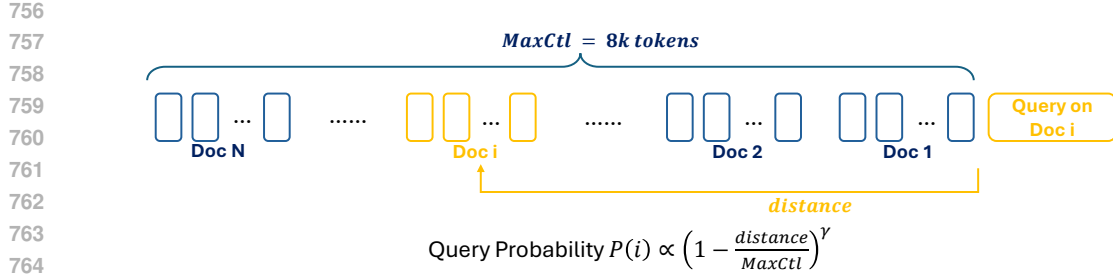


Figure 8: Our modified Position-Weighted Ruler-QA1 (Hsieh et al., 2024) dataset. Multiple paragraphs are concatenated together with context length close to  $MaxCtl$ , and a question queries the ‘golden paragraph’ (i.e. the doc paragraph with answer to that query). In the original Ruler-QA1 dataset each doc has equal probability of being queried (i.e.  $\gamma = 0$ ); while in our experiments shown in Figure 9, we measure LLM performance on a set of tasks with different hyper-parameter  $\gamma$ , each with different probability of querying far-away contexts.

## A DOWNSTREAM TASK

In the main paper, we experimentally discover and theoretically analyze how context length impact Cross Entropy loss for next token prediction. Previous studies (Hsieh et al., 2024) show that Cross Entropy Loss might not be highly correlated with important downstream tasks.

In this section, we study the impact of context length on downstream document QA tasks, similar to those proposed in Ruler-QA1 (Hsieh et al., 2024). The conclusions we observe in this section are:

- 1. For downstream tasks studied (i.e. similar to Ruler-QA document QA tasks), optimal context length still exists, and this phenomena can be analyzed from the perspective of Bayes Risk and Approximation Loss.
- 2. For these tasks, Intrinsic Entropy can still act as a proxy of information learned, and when Language Model is not deviating from Bayes Model by a large margin, is still positively-correlated with QA accuracy.

## A.1 OPTIMAL CONTEXT LENGTH ON RULER-QA: A CASE STUDY

Ruler-QA1 (Hsieh et al., 2024) is representative among a series of doc-QA tasks in the sense that (1) it is composed of real-world documents and QA pairs from Doc-QA tasks like SQuAD (Rajpurkar et al., 2016); (2) its samples are generated by inserting a ‘golden paragraph’ (i.e. the paragraph containing answer to a specific question in SQuAD) into other paragraphs sampled also from SQuAD, hence one can control the total length of tested samples. This provides us with a great testbed for experimenting the impact of visible context length to models, and to test the Intrinsic Entropy. The task shown in Figure 8 (with  $\gamma = 0$  setting) aligns with the Ruler-QA1 dataset.

We study the performance of Llama-3.1-8B. For the original Ruler-QA1 dataset, the ‘golden paragraph’ is inserted randomly and uniformly across the sample. We first generate samples with  $max\_ctl = 16k$ , i.e. each sample has length close to 16k tokens and is composed of multiple paragraphs sampled from SQuAD, and we test the Language Model to answer a question related to some certain paragraph uniformly distributed across the context. During test, we only allow the Language Model to see the closest ‘ctl’ tokens (and hence it cannot see previous paragraphs), and measure accuracy varying this ‘ctl’. The result is shown in the line labeled as ‘uniform distributed’ in Figure 9. As shown, though the accuracy first increases when increasing context length, but the context length drops after  $ctl = 6k$ . This proves the existence of an optimal context length, for Llama-3.1-8B on Ruler-QA1.

To further study how this optimal context length depends on the property of tasks, we propose the Position-Weighted Ruler-OA1 dataset. We test the Language Model to answer a question related

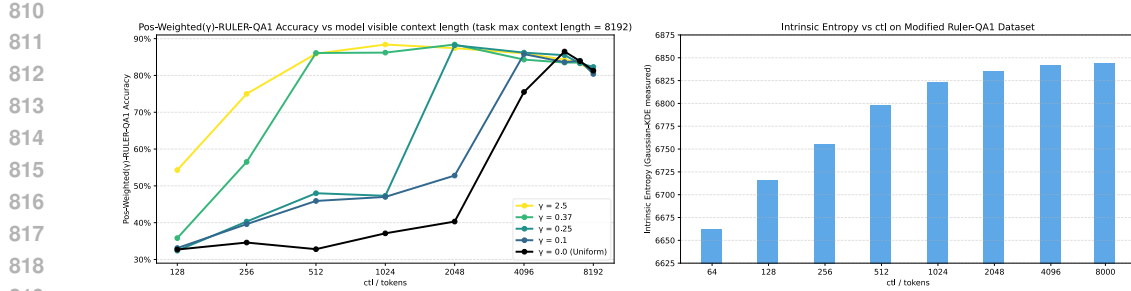


Figure 9: **Measured results on Position-Weighted Ruler-QA1 dataset.** **Left:** QA accuracy v.s. number of tokens input to the Language Model, for different tasks with different  $\gamma$  values. We observe that: (1) each curve shows a trend to increase and then decrease with context length; and (2) the critic point corresponds to a smaller optimal context length for tasks with larger  $\gamma$  (i.e. tasks requiring less long context abilities). **Right:** Intrinsic Entropy measured on samples truncated to certain context lengths. The Intrinsic Entropy shows increment of intrinsic information when increasing context length, and resembles acc-ctl curves for larger  $\gamma$ .

to a certain paragraph sampled by:  $P(x) \propto (1 - x/L)^\gamma$ , where  $x$  is the distance of the paragraph to end of input (in tokens),  $L$  is the maximum context length (i.e.  $8k$ ), and  $\gamma$  is a hyper-parameter, fixed for certain task.  $\gamma = 0$  degrades to uniform distribution (i.e. the standard Ruler-QA1 task), while a larger  $\gamma$  means the task focuses less on far-away tokens. Similarly, for a fixed  $\gamma$ , we adjust the number of tokens visible to Language Models ('ctl') and measure its accuracy; results are also shown in Figure 9. From the figure, we have two observations: (1) an optimal context length exists for each  $\gamma$ ; and (2) a smaller  $\gamma$  (i.e. task requires more long context) typically leads to a larger optimal context length.

This result can also be analyzed from the Bayes Risk and Approximation Loss decomposition perspective. Intuitively, some tasks require larger context lengths to solve (i.e. the Bayes Risk of that metric decreases slower with context length compared to other tasks like Cross Entropy loss for next token prediction), thus they need more contexts. However, since the model's performance would decrease for long contexts after all (i.e. the Approximation Loss still increases with context length), the balance of these two terms still leads to an optimal context length. In main paper, we fixed task, vary training set size, and show optimal context length increases with training budget and dataset size; in this appendix section, we fix the model (so we fix training budget and dataset as well), and show optimal context length increases with (downstream) tasks' typical context length.

## A.2 INTRINSIC ENTROPY: A PROXY OF INFORMATION LEARNED BY LANGAUGE MODEL

We measure Intrinsic Entropy of different context length on the Doc paragraphs samples we construct. In our experiment, we take the closest  $ctl$  tokens of the concatenated samples as input to Language Model (Llama-3.1-8B), and take the hidden state of the final layer of a close-to-the-end token. After obtaining  $N$  such vectors, we conduct Gaussian-KDE to measure the Intrinsic Entropy. The result is shown in the right figure of Figure 9.

We observe from Figure 9 that, the Intrinsic Entropy still increases as the input context length increases. Moreover, though measured Intrinsic Entropy does not always follow a linear relationship with QA accuracy (notice that the Intrinsic Entropy calculated does **not** depends on  $\gamma$ , while QA accuracy is related to the task setting  $\gamma$ ), we still see a positive correlation between Intrinsic Entropy and QA accuracy when context length is not very long.

In principal, a drop in accuracy when increasing context length actually implies that the model is no longer a good approximation of Bayes Model for certain task at that context length. For relatively larger  $\gamma$  tasks (i.e. tasks focusing more on nearer tokens), we see a more aligned trend in increment of QA accuracy and Intrinsic Entropy; while for smaller  $\gamma$  tasks (those focusing on farther tokens), the QA accuracy might increase a lot when Intrinsic Entropy increases a little. This potentially implies that Language Models are memorizing and keeping only the information likely to be useful from farther-away tokens, and these pieces of information are sufficient for the QA task.

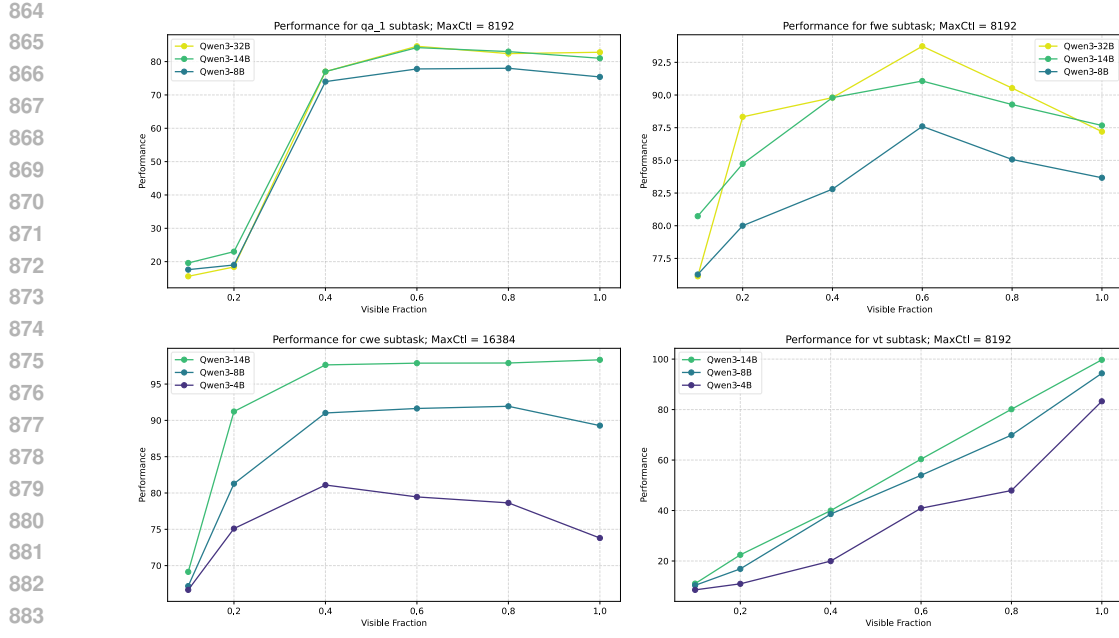


Figure A.3-1. Acc v.s. Visible Context Length of Qwen-3 series models (non-thinking chat models) on 4 representative subsets of the RULER dataset: qa\_1 (**document qa, upper-left**), fwe (**frequent word extraction, upper-right**), cwe (**common words extraction, lower-left**), and vt (**variable tracking, lower-right**), for a fixed max context length and a varying visible fraction of the input context. Most models show an optimal context length for qa\_1, fwe and cwe subtask, while the vt subtask shows increased performance with respect to context length. Moreover, larger model tends to perform better and have a larger optimal context length, represented by the performance comparison between Qwen3-4B and Qwen3-8B on cwe subtask (lower-left).

### A.3 MORE EXPERIMENTS ON RULER BENCHMARK

To see how different tasks might have different behaviors with respect to context length, we further conduct experiments on three RULER subtasks: the qa1 subtask (document qa), the cwe subtask (i.e. common words extraction), the vt subtask (i.e. variable tracking), and the fwe subtask (i.e. frequent words extraction). Other subtasks like single-needle-in-haystack are too simple for sota LLMs hence we did not perform experiments on them.

To study the impact of model size, we utilize the Qwen3 series models. We use the non-thinking mode of the chat models of Qwen3 series Yang et al. (2025), including Qwen3-4B, Qwen3-8B, QWen3-14B and Qwen3-32B for experiments. We use codebase modified from RULER Hsieh et al. (2024). The maximum context length is set to 16k for cwe and 8k for other subtasks. These results are shown in Figure A.3-1.

As shown in Figure A.3-1, (1) for subtasks resembling fwe, document qa, variable tracing, etc., there exists an optimal context length for most models tested; and (2) for vt (variable tracking), in the experiment we conducted models' performance improve with respect to visible context fraction. This could be caused by the fact that variable tracking is relatively easy for current LLMs, thus their approximation loss is low; while given its distribution of variables the Bayes Risk would constantly decrease with more context length, thus it shows a trend of improving even for long visible fraction.

Comparing the results of Qwen3-4B, Qwen3-8B and Qwen3-14B on the cwe subtask in Figure A.3-1, we see that: (1) **optimal context length is larger and harder to observe for larger models**, this can be attributed to larger models lead to less Approximation Loss; comparing results of the same cwe subtask on different max context lengths in Figure A.3-2, we see that: (2) **optimal context length is easier to observe for longer task**, which can also be attributed to a larger Approximation Loss (i.e. language models fall short to deal with longer contexts).

918

919

920

921

922

923

924

925

926

927

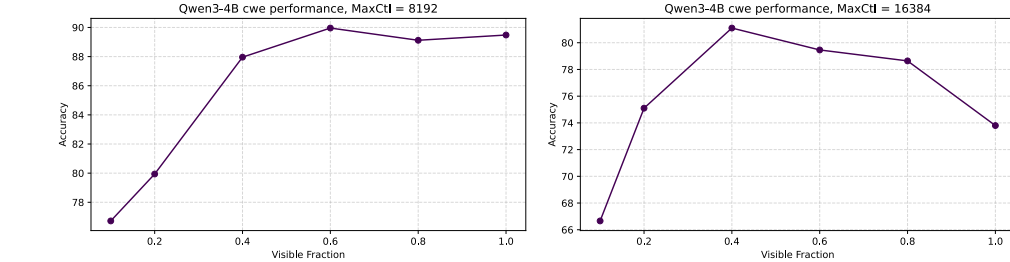


Figure A.3-2. Acc v.s. Visible Context Length of Qwen-3 4B, on cwe (common words extraction) subtask, with different Max context length (**left**:  $MaxCtl = 8k$ , **right**:  $MaxCtl = 16k$ ). As shown, though optimal context length is hard to observe for the task requiring  $8k$  as max context length, it is easy to observe for that requiring  $16k$  as max context length.

These results could potentially argue that the subtasks defined in RULER are of different difficulty for current LLMs. That is, if one can observe an optimal context length, this proves that the model **gets distracted** by more context beyond the optimal context length, and hence performance gets worse even if these context contains more information. **Potentially, our work provides a new perspective:** Consider a case where some specific LM achieves 95% accuracy on certain subtask with 0.8 visible context fraction and 90% accuracy on it with 1.0 visible context fraction. Even though the absolute accuracy numbers are high, the existence of optimal context length and degraded performance also implies an ineffectiveness of the language model when handling long contexts with respect to that specific task.

## B DEFINITION AND PROPERTIES OF CROSS ENTROPY LOSS

### B.1 DEFINITION OF CROSS ENTROPY LOSS DISCUSSED IN THIS WORK

It is well-known that the original definition of Cross Entropy between two sequential distributions  $P$  and  $Q$ :  $H_{org}(P, Q)$  should be:

$$\begin{aligned}
 H_{org}(P, Q) &= \sum_x -P(x) \log Q(x) \\
 &= \sum_x -P(x_{-\infty:0}) P(x_0|x_{-\infty:0}) \\
 &\quad * \log\{Q(x_0|x_{-\infty:0})Q(x_{-\infty:0})\},
 \end{aligned}$$

where  $x_{a:b}$  denotes  $x_a, x_{a+1}, \dots, x_{b-1}$ ; it is common practice to calculate perplexity of Language Models with its input as GT labels (e.g. in technical report of LLaMa-3(Grattafiori et al., 2024)), in other words, the experimentally measured Cross Entropy  $H_{exp}(P, Q)$  is actually:

$$\begin{aligned}
 H_{exp}(P, Q) &= \sum_x -P(x_{-\infty:1}) \log \{Q(x_0|x_{-\infty:0})\mathbf{P}(\mathbf{x}_{-\infty:0})\} \\
 &= \text{Const} + E_{x_{-\infty:0}} \sum_{x_0} -P(x_0|x_{-\infty:0}) \log Q(x_0|x_{-\infty:0}).
 \end{aligned}$$

Therefore, in this work we use:

$$\begin{aligned}
 &H(P, Q) \\
 &= H_{exp}(P, Q) \\
 &= E_{x_{-\infty:0}} \left[ \sum_{x_0} -P(x_0|x_{-\infty:0}) \log Q(x_0|x_{-\infty:0}) \right]
 \end{aligned} \tag{7}$$

972 as the definition of Cross-Entropy loss, and  $P(x_0|x_{-\infty:0})$ ,  $Q(x_0|x_{-\infty:0})$  as the definition of Nature  
 973 Language distribution and Language Model distribution, respectively.  
 974

## 975 B.2 CROSS ENTROPY LOSS FOR LANGUAGE MODEL WITH CONTEXT LENGTH $l$

977 In Equation B.1, if  $Q_l(x_0|x_{-\infty:0})$  is a language model with limited context length  $l$ :  
 978  $Q_l(x_0|x_{-\infty:0}) = Q_l(x_0|x_{-l:0})$ , we have:  
 979

$$\begin{aligned}
 & H(P, Q_l) \\
 &= E_{x_{-\infty:0}} \left[ \sum_{x_0} -P(x_0|x_{-\infty:0}) \log Q_l(x_0|x_{-l:0}) \right] \\
 &= - \sum_{x_{-\infty:1}} P(x_{-\infty:1}) \log Q_l(x_0|x_{-l:0}) \\
 &= - \sum_{x_{-\infty:-l}} \sum_{x_{-l:1}} P(x_{-\infty:-l}, x_{-l:1}) \log Q_l(x_0|x_{-l:0}) \\
 &= - \sum_{x_{-l:1}} P(x_{-l:1}) \log Q_l(x_0|x_{-l:0}) \\
 &= E_{x_{-l:0}} \left[ \sum_{x_0} -P(x_0|x_{-l:0}) \log Q_l(x_0|x_{-l:0}) \right] \\
 &= H(P_l, Q_l).
 \end{aligned}$$

996 Note that  $P(x_0|x_{-l:0})$  is exactly the Bayes Model with context length  $l$ . Hence, we have:  
 997

$$\begin{aligned}
 D_{KL}(P, Q_l) &= -H(P) + H(P, Q_l) \\
 &= -H(P) + H(P_l, Q_l) \\
 &= -H(P) + H(P_l) + D_{KL}(P_l, Q_l).
 \end{aligned}$$

1003 Specially, if we are calculating the KL Divergence between Nature Language and Bayes Model with  
 1004 context length  $l$ , thus  $Q_l = P_l$ , we have:  
 1005

$$D_{KL}(P, P_l) = -H(P) + H(P_l, P_l) = -H(P) + H(P_l). \quad (8)$$

## 1009 C EXPERIMENTALLY MEASURE NEXT-TOKEN-PREDICTION INFORMATION 1010 ENTROPY $S_{ntp}$

### 1013 C.1 PCA-BASED INFORMATION ENTROPY ESTIMATION

1015 Though related, Entropy in Intrinsic Space does not equal to Entropy in the next token prediction  
 1016 task. From the probability perspective, let  $dec(x)$  be the next decoded token for some point  $x$  in the  
 1017 intrinsic space, we have:  $S = \sum_{x \in IS} -P(x) \log P(x)$ , while  $S_{ntp} = -\sum_{v \in vocab} P(v) \log P(v)$   
 1018 where  $P(v) = \sum_{x \in IS, dec(x)=v} P(x)$ .  $S_{ntp}$  is a coarse-grained Entropy compared to  $S$ .  $S$  contains  
 1019 important information on previous tokens that are important for the prediction of future tokens, while  
 1020  $S_{ntp}$  is related only to the next token.

1021 Experiments in Figure ?? show that, no matter what subspace we use, the Cross Entropy Loss  
 1022 usually follows a linear relationship with the Entropy we measured in the subspace, **supporting the**  
 1023 **claim that the next token prediction task likely lies in some subspace of the Intrinsic Space, or**  
 1024 **(statistically) its Entropy should be some weighted average of Entropy of several subspaces of**  
 1025 **similar dimension.** This also suggests that  $H_{ntp}$  is approximately linear with  $H_{IS}$ , which validates  
 our previous assumptions and claims.

1026  
1027

## C.2 GAUSSIAN-KDE BASED INFORMATION ENTROPY ESTIMATION

1028  
1029  
1030  
1031

In this sub-subsection we use another method for Information Entropy Estimation. As shown in Figure 10, this estimation also aligns well with PCA-based estimation; moreover, such estimated entropy is also linear with respect to Intrinsic Dimension and Cross Entropy Loss.

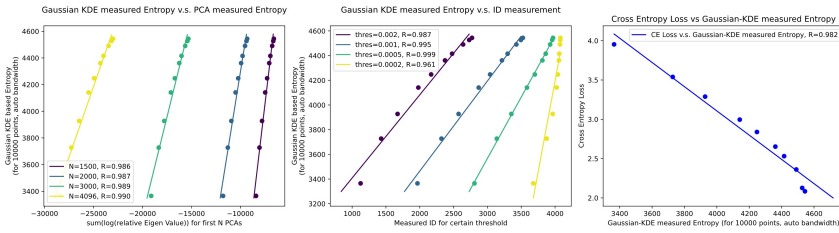
1032  
1033  
1034  
1035  
1036  
1037  
1038  
10391040  
1041  
1042  
1043  
1044

Figure 10: Gaussian-KDE measured Entropy (10000 samples, auto bandwidth = 0.997756) v.s. PCA-measured Entropy (left), Measured ID (middle) and Cross Entropy Loss (right).

1045  
1046

## C.3 SYNTHETIC DATASET: ENTROPY IN INTRINSIC SPACE, AND ENTROPY FOR OUTPUT LAYER

1047  
1048  
1049  
1050  
1051

For our synthetic dataset, if we view the **Context Feature Vector** shown in **Figure 16** as the feature in the Intrinsic Space, then the best strategy for the context encoder is to generate the answer for all subtasks (it can see) in the Intrinsic Space (since it cannot see the task bits). This would lead to an Entropy of  $S = T \log 2$  in the Intrinsic Space.

1052  
1053  
1054  
1055  
1056

The entropy of the output layer is, however,  $S_{output} = \log 2$  since the answer bits 0, 1 have the same probability. In this way, the answer of the output layer actually corresponds to one dimension in the Intrinsic Space, which should be the exact dimension at which the answer of the current task is stored. Therefore,  $S_{output} = 1/T * S_{IS}$ , which explains why the Entropy for output logits is linear to the Entropy for Intrinsic Space.

1057

## C.4 DETAILS FOR SYNTHETIC DATA

1058

Here we present details for synthetic dataset and model training.

1059  
1060  
1061  
1062  
1063

We use 100 tasks and 60 task bits. From 11<sup>th</sup> to the 60<sup>th</sup> bit, each bit corresponds to the max bit of two tasks: that is,  $\#\text{Task}|_{\max(\text{bit}_1, \text{bit}_2)=i} = 2, \forall i \in \{11, 12, \dots, 60\}$ .

1064  
1065  
1066  
1067  
1068  
1069

During training, 50% of the samples are unmasked, while for the other 50% samples, we mask the last  $X$  task bits to be 0.5, where  $X$  is a random int from 60 – 10 to 60 – 60. This ensures our model to be able to handle mask bits, and also ensures it can learn uncommon tasks (relying on context bits that are at the end of the context bits) well. We train the model on a training set of 10000000 and a validation set of size 1000000, for 125 epochs (and an early stopping setting of 25 epochs, though the training process did not trigger early stopping).

1070  
1071  
1072  
1073  
1074  
1075

To make sure that the trained model can be used to approximate the Bayes Model, we compare the model’s loss on validation set with context  $ctl$  with the calculated minimum possible CE Loss for the task. As shown in Table 1 that the model is not too different from the Bayes Model: the BCE Loss only differs by around 0.001. **Thus, we can use the middle-representation (shown as context feature in Figure 6) as the feature in Intrinsic Space to approximate the Bayes Model for  $17 \leq ctl \leq 50$ .**

1076  
1077  
1078  
1079

$$\text{MinCELoss}(ctl) = \left( \sum_{\text{task s.t. } \max(\text{bit}_1, \text{bit}_2) > ctl} \text{freq}(\text{task}) * \log 2 \right) / \sum_{\text{task}} \text{freq}(\text{task})$$

1080	Context Length	Model CE Loss	Minimum CE Loss Calculated
1081	17	0.4648	0.4643
1082	20	0.3988	0.3988
1083	23	0.3438	0.3437
1084	25	0.3119	0.3116
1085	28	0.2687	0.2686
1086	30	0.2429	0.2429
1087	35	0.1867	0.1864
1088	40	0.1390	0.1387
1089	50	0.0613	0.0612

1091  
1092 Table 1: Comparison between trained model and Bayes Model (minimum CE Loss) for Synthetic  
1093 Data

## 1094 D DEFINITIONS OF INTRINSIC SPACE AND DERIVED PROPERTIES

1097 As mentioned in Section 2.1.2, in previous work (Bahri et al., 2024; Cheng et al., 2023), as a common  
1098 practice, the ‘Data Manifold’ is often **defined** as the middle feature representation of well-trained  
1099 neural networks, and **assumptions** are made on this kind of mid-representation, with experiments to  
1100 **validate** these assumptions. (Intrinsic Space is defined as the space where the Data Manifold lies.)

1101 Meanwhile, the Data Manifold can be more formally **defined** by a mapping from input data to some  
1102 Intrinsic Space which satisfies a certain set of **properties**, and mid-representation of well-trained  
1103 neural networks are **assumed to have such properties**, which can be experimentally **validated**.  
1104 These two perspectives are actually equivalent to each other:

- 1105 • **Perspective 1:** Experiments show mid-representations of neural networks have certain  
1106 properties → Data Manifold in Intrinsic Space satisfies such properties.
- 1107 • **Perspective 2:** Experiments show mid-representations of neural networks have certain  
1108 properties → such mid-representation can be viewed as Data Manifold of Intrinsic Space  
1109 that is defined to have such properties.

1111 These two perspectives are equivalent to each other, and Perspective 1 is used in some previous  
1112 work (Bahri et al., 2024; Sharma & Kaplan, 2022).

1113 In this section, we formally define the Intrinsic Space and formally derive related results, following  
1114 **Perspective 2**.

### 1116 D.1 FORMAL DEFINITIONS OF INTRINSIC SPACE

1118 We define an *intrinsic space* to formalize the latent structure underlying natural language sequences.  
1119 This space is independent of surface forms and aims to capture the semantic and syntactic essence  
1120 of language contexts across different sequence lengths.

1122 **Setup.** Let  $\mathcal{V}$  be a finite vocabulary and  $\mathcal{X} = \mathcal{V}^*$  the set of all finite sequences over  $\mathcal{V}$ . Let  $\mathcal{M} \subset \mathcal{X}$   
1123 denote the *original data manifold* of natural language, i.e., the support of the data distribution  $p(x)$ .

1125 **Definition.** An **intrinsic space**  $\mathcal{Z}$  is a latent representation space defined by a mapping

$$1126 \Phi : \mathcal{X}_{\leq t} \rightarrow \mathcal{Z}, \quad (9)$$

1127 where  $\mathcal{X}_{\leq t} = \bigcup_{k=0}^t \mathcal{V}^k$  is the set of all language contexts of length  $t$ . The image of the *original*  
1128 *data manifold* under this map is denoted  $\mathcal{M}_{\mathcal{Z}} = \Phi(\mathcal{M}_{\leq t}) \subset \mathcal{Z}$ , or the *data manifold* (in Intrinsic  
1129 Space). We require the following properties:

- 1131 • **Predictive Consistency:** There exists a decoder  $\pi : \mathcal{Z} \rightarrow \Delta(\mathcal{V})$  such that

$$1132 \pi(\Phi(x_{\leq t})) = p(x_t | x_{\leq t}), \quad (10)$$

1133 i.e., the intrinsic representation enables accurate next-token prediction.

1134 Moreover, there are some other properties assumed (separately) in our work, for which we give a  
 1135 formal definition here.  
 1136

- **Uniform Information Gain:** This assumption assumes the following linear relationship between predictive divergence and intrinsic dimension  $\dim(l)$ :

$$D_{KL}(P, P_l) = s \cdot (\dim(\infty) - \dim(l)) \quad (11)$$

1140 for some constant  $s > 0$ , which we interpret as the average number of bits of predictive  
 1141 information contributed by each intrinsic dimension. This is empirically observed in ex-  
 1142 periments.  
 1143

- **Linear Entropy Relationship** This assumption assumes that there exists constant  $0 < s < 1$ ,  $b$  and a sequence of tolerances  $\{\varepsilon_t\}_{t \geq 0}$  with  $\varepsilon_t \rightarrow 0$  such that for every context length  $t$ ,

$$| -s H[q_t(Z)] + b - H[p(\cdot | x_{<t})] | \leq \varepsilon_t. \quad (12)$$

1146 Where  $q_t(\cdot)$  denotes probability density function. Equivalently, in the idealized zero-  
 1147 tolerance limit:

$$-s H[q_t(Z)] + b = H[p(x_t | x_{<t})] \quad \forall t. \quad (13)$$

1148 It is worth mentioning that, we can easily derive the linear entropy relationship from the  
 1149 uniform information gain assumption, but not vice versa. Hence, linear entropy relationship  
 1150 is a *weaker* assumption compared to uniform information gain.  
 1151

- **Lipschitz Differentiable Density** This assumption assumes the density of data distribution is smooth in the intrinsic space:

$$\|\nabla q(z)\| \leq L \quad (14)$$

1152 for some constant  $L > 0$   
 1153

- **Finite  $\epsilon$ -negative moment:** This assumption means the integral of the  $\epsilon$ -negative moment of the data distribution is finite:

$$\int_{\mathcal{Z}} q(z)^{1-\epsilon} dz := C_\epsilon < \infty. \quad (15)$$

1154 Remark. When  $\mathcal{Z}$  is bounded ( $\int_{\mathcal{Z}} q(z) dz = V_{\mathcal{Z}} < \infty$ ), and if there exists a constant  
 1155  $q_{min} > 0$  s.t.  $q(z) \geq q_{min} > 0$ , then this assumption is satisfied. Hence this is a weaker  
 1156 assumption compared to boundedness and non-zero density, which is even weaker than  
 1157 uniform distribution assumption.  
 1158

	Key Properties Assumed	Derived Results
(Bahri et al., 2024) Theorem 2	Bounded, Uniform Distribution, Lipschitz Differentiable	Data Scaling for Approx. Loss
Theorem 1, 2 in Appendix D.2 (corr. to Section 2.3)	(Bounded,) Finite Negative Moment, Lipschitz Differentiable	Data Scaling for Approx. Loss
Theorem 3 in Appendix D.3 (corr. to Section 2.2.1)	Predictive Consistency, Uniform Information Gain	Bayes Risk for Ntp of varied Ctl (Intrinsic Dimension perspective)
Theorem 4 in Appendix D.4 (corr. to Section 2.2.1)	Predictive Consistency, Linear Entropy Relationship	Bayes Risk for Ntp of varied Ctl (Information Entropy perspective)

1159 **Table 2: In this Section (Appendix D) we formulate results from previous sections with The-  
 1160orems derived with defined assumptions and properties of intrinsic space in this section.** Ntp  
 1161 refers to Next-token-prediction, Ctl refers to Context Length. We derive data scaling for approxima-  
 1162 tion loss with weaker assumptions compared to (Bahri et al., 2024), please refer to Theorem 1, 2 in  
 1163 Appendix D.2 for more details.  
 1164

1165 To conclude: if some space satisfies these properties, then the data representation is referred to as  
 1166 ‘Data Manifold’ in this space, and such properties would lead to further derivations in these work  
 1167 (including this work). In experiments, Middle-representation of neural networks are assumed (and  
 1168 shown) to have these kind of properties, hence explain some of the scaling behaviors they have.  
 1169

1188  
1189

## D.2 DERIVATION FOR DATA SCALING FOR APPROXIMATION LOSS

1190  
1191  
1192

**Theorem 1** (Expected capped nearest-neighbour distance). *Let  $\mathcal{Z} \subseteq \mathbb{R}^d$  ( $d \geq 1$ ) and there exists a non-empty open set  $U \in \mathbb{R}^d$  such that  $U \subseteq \mathcal{Z}$  (i.e.,  $\mathcal{Z}$  is a  $d$ -dimensional region). Let  $q : \mathcal{Z} \rightarrow [0, \infty)$  be a probability density satisfying*

1193  
1194  
1195  
1196  
1197

1. **Lipschitz Differentiable:**  $\|\nabla q(z)\| \leq L$  for all  $z \in \mathcal{Z}$ ;

2. **Finite  $\epsilon$ -negative moment:** for some fixed  $\epsilon > 1/d$ ,  $\int_{\mathcal{Z}} q(z)^{1-\epsilon} dz := C_{\epsilon} < \infty$ .

1198

Draw i.i.d. samples  $\mathcal{Z}_D = \{Z_1, \dots, Z_D\} \sim q^{\otimes D}$  and define the capped nearest-neighbour distance

1199  
1200

$$R_M(Z_i) = \min\{M, \min_{j \neq i} \|Z_i - Z_j\|\}, \quad M > 0. \quad (16)$$

1201  
1202  
1203

Then, there exists constant  $C = C(d, L, \epsilon, M, C_{\epsilon})$  and  $D_0 = D_0(d, L, \epsilon, M, C_{\epsilon})$  such that  $\forall D > D_0$ :

1204  
1205  
1206  
1207

$$\mathbb{E}_{\mathcal{Z}_D}[R_M(Z_1)] \leq \begin{cases} C (\log D)^{\epsilon/(d+1)} D^{-\epsilon/(d+1)}, & \text{if } \epsilon < \frac{d+1}{d}, \\ C D^{-1/d}, & \text{if } \epsilon \geq \frac{d+1}{d}. \end{cases} \quad (17)$$

1208

Thus, there exists constant  $c = c(L, \epsilon, M, C_{\epsilon})$ , such that:

1209  
1210

$$\mathbb{E}_{\mathcal{Z}_D}[R_M(Z_1)] \leq C D^{-c/d}. \quad (18)$$

1211  
1212  
1213  
1214

*Proof.* We write  $Z_1$  for the distinguished point and  $R(Z_1) = \min_{j \neq 1} \|Z_1 - Z_j\|$  for its exact nearest-neighbour distance, always capping by  $M$  at the very end. Throughout the proof the expectation  $\mathbb{E}[\cdot]$  is taken over the whole sample  $\mathcal{Z}_D = (Z_1, \dots, Z_D) \sim q^{\otimes D}$ .

1215  
1216

### Step 0. Notation.

1217  
1218  
1219

$$v_d := \text{vol}(B_1(0)), \quad c_d := \frac{v_d}{2}, \quad r_0(z) := \frac{q(z)}{2L}.$$

1220  
1221

$v_d$  is the volume of a unit ball. Moreover, since  $\|\nabla q\| \leq L$ , whenever  $r \leq r_0(z)$  one has  $q(u) \geq \frac{1}{2}q(z)$  for every  $u \in B_r(z)$ .

1222

### Step 1. Exponential hole probability inside the Lipschitz ball.

1224  
1225

Fix  $z$  and  $r \leq r_0(z)$ . The *mass* of  $q$  inside  $B_r(z)$  satisfies

1226  
1227

$$\mu_r(z) := \int_{B_r(z)} q(u) du \geq \frac{1}{2} q(z) v_d r^d = c_d q(z) r^d.$$

1228  
1229  
1230

Conditioned on  $Z_1 = z$ , the  $(D-1)$  other points are i.i.d.  $q$ , so the conditional probability that all other points are sampled outside the ball  $B_r(z)$  is:

1231  
1232

$$\Pr(R(z) > r \mid Z_1 = z) = (1 - \mu_r(z))^{D-1} \leq \exp[-c_d(D-1)q(z)r^d]. \quad (19)$$

1233

### Step 2. Density threshold and spatial split.

1234  
1235  
1236

Define a data-dependent threshold

1237  
1238

$$\lambda_D := \left( \frac{2^{d+1} L^d d \log D}{c_d D} \right)^{\frac{1}{d+1}} \quad (D \geq 2), \quad \mathcal{H}_D := \{z : q(z) \geq \lambda_D\}, \quad \mathcal{L}_D := \mathbb{R}^d \setminus \mathcal{H}_D.$$

1239  
1240  
1241

(The power  $1/(d+1)$  is tuned to balance two error terms below.)

### Step 3.1. Distribution in $\mathcal{H}_D$ (moderate or high density region).

1242 For every  $z \in \mathcal{H}_D$  set

$$1243 \quad 1244 \quad 1245 \quad \rho(z, D) := \left( \frac{2d \log D}{c_d D q(z)} \right)^{1/d}.$$

1246 *Bound on  $\rho$ .* Since  $q(z) \geq \lambda_D$ ,  $\rho(z, D) \leq r_0(z)$  and therefore equation 19 is valid for all  $0 < r \leq$   
1247  $\rho(z, D)$ .

1248 *Tail probability at  $\rho$ .* With  $r = \rho(z, D)$ ,

$$1249 \quad 1250 \quad \Pr(R(z) > \rho(z, D) \mid Z_1 = z) \leq \exp[-2d \log D] = D^{-2d}.$$

1251 Because  $R_M(Z_1) = \min(R(Z_1), M) \leq M$ ,

$$1252 \quad 1253 \quad \mathbb{E}[R_M(Z_1) \mathbf{1}_{\{R > \rho\}} \mid Z_1 = z] \leq M D^{-2d}. \quad (20)$$

1254

1255 *Integral of  $R$  up to  $\rho$ .* Using equation 19,

$$1256 \quad 1257 \quad \mathbb{E}[R(Z_1) \wedge \rho(z, D) \mid Z_1 = z] = \int_0^\rho \Pr(R > r \mid Z_1 = z) dr \\ 1258 \quad 1259 \quad \leq \int_0^\rho \exp[-c_d(D-1)q(z)r^d] dr.$$

1260 Make the change of variable  $t := c_d(D-1)q(z)r^d$ ; then  $r = (t/c_d(D-1)q(z))^{1/d}$  and  $dr =$   
1261  $\frac{1}{d}r dt/t$ . The upper limit  $r = \rho$  maps to  $t = 2d \log D$ . Hence

$$1262 \quad 1263 \quad \int_0^\rho \exp[-c_d(D-1)q(z)r^d] dr = \frac{\Gamma(1+1/d)}{d^{1/d} c_d^{1/d}} (Dq(z))^{-1/d}.$$

1264 Absorbing constants:

$$1265 \quad 1266 \quad \mathbb{E}[R(Z_1) \wedge \rho(z, D) \mid Z_1 = z] \leq C_{d,L} (Dq(z))^{-1/d}. \quad (21)$$

1267 *Average over  $z \in \mathcal{H}_D$ .* Taking expectation over  $Z_1$  first restricted to  $\mathcal{H}_D$  and then combining  
1268 equation 21 with equation 20,

$$1269 \quad 1270 \quad \mathbb{E}[R_M(Z_1) \mathbf{1}_{\mathcal{H}_D}(Z_1)] \leq C_1 D^{-1/d} + M D^{-2d}, \quad C_1 := C_{d,L} (\mathbb{E}[q(Z)^{-1/d}])^{1/d} < \infty. \quad (22)$$

### 1271 Step 3.2. Distribution in $\mathcal{L}_D$ (ultra-low density region).

1272 On  $\mathcal{L}_D$  one has  $q(z)^\epsilon \leq \lambda_D^\epsilon$ , so by Hölder's inequality

$$1273 \quad 1274 \quad \Pr(Z \in \mathcal{L}_D) = \int_{q < \lambda_D} q(z) dz \leq \lambda_D^\epsilon \int_{\mathbb{R}^d} q(z)^{1-\epsilon} dz = C_\epsilon \lambda_D^\epsilon.$$

1275 Since  $R_M \leq M$ ,

$$1276 \quad 1277 \quad \mathbb{E}[R_M(Z_1) \mathbf{1}_{\mathcal{L}_D}(Z_1)] \leq M C_\epsilon \lambda_D^\epsilon = M C_\epsilon (\log D)^{\epsilon/(d+1)} D^{-\epsilon/(d+1)}. \quad (23)$$

1278

### 1279 Step 4. Global bound.

1280 Adding equation 22 and equation 23. For large enough  $D$ , the term  $M D^{-2d}$  is higher-order small  
1281 quantity compared to  $D^{-1/d}$  or  $D^{-\epsilon/(d+1)}$ . Therefore,

$$1282 \quad 1283 \quad \mathbb{E}[R_M(Z_1)] \leq C_1 D^{-1/d} + M C_\epsilon (\log D)^{\epsilon/(d+1)} D^{-\epsilon/(d+1)} + o(\min(D^{-1/d}, D^{-\epsilon/(d+1)})).$$

1284 Finally, compare the two powers of  $D$ . If  $\epsilon < \frac{d+1}{d}$  then  $\epsilon/(d+1) < 1/d$  and the second term  
1285 dominates; otherwise the first dominates. This yields the two-case estimate claimed.  $\square$

1296 **How large can  $\epsilon$  be, for unbounded and bounded  $\mathcal{Z}$ ?**  
1297

1298 • **It is usually assumed (Bahri et al., 2024; Sharma & Kaplan, 2022) that  $\mathcal{Z}$  is bounded:**  
1299 this assumption makes sense since in usual cases we approximate Intrinsic Space with mid-  
1300 dle feature representation of neural networks, which can indeed be bounded. For bounded  
1301  $\mathcal{Z}$ , it is possible for  $\epsilon$  to be larger than  $1 + 1/d$ . We would like to mention that in (Bahri  
1302 et al., 2024), a constant distribution  $q(z) = \text{Const}$  is assumed, where  $\epsilon$  can be arbit-  
1303 rarily large and dominant rate  $D^{-1/d}$  is derived: this is a much stronger assumption  
1304 compared to Finite  $\epsilon$ -negative moment we assumed in our work.

1305 • **If  $\mathcal{Z}$  is bounded and  $\exists q_{min} > 0$  such that  $\forall z, q(z) \geq q_{min} > 0$ , then  $\forall z > 1$ ,**  
1306  $\int_{\mathcal{Z}} q(z)^{1-\epsilon} dz \leq \int_{\mathcal{Z}} q_{min}^{1-\epsilon} dz = q_{min}^{1-\epsilon} \int_{\mathcal{Z}} dz$ , and the final term is finite for any  $\epsilon$ . That  
1307 is, in this case  $\epsilon$  can be arbitrarily large.

1308 • For unbounded  $\mathcal{Z}$ ,  $\epsilon < 1$  is the usual case; at  $\epsilon = 1$  the condition becomes  $\int q^0 =$   
1309  $\text{Leb}(\text{supp } q) < \infty$ , i.e. *compact support of finite measure*. For most unbounded densi-  
1310 ties (Gaussians, sub-exponential, power-law) one only has  $\epsilon < 1$ .

1311 • The comparison threshold  $\frac{d+1}{d}$  is always  $> 1$  when  $d \geq 1$ ; hence the dominant rate is

$$\begin{cases} D^{-\epsilon/(d+1)} & \text{for every admissible } 1/d < \epsilon < 1, \\ D^{-1/d} & \text{only if the support is compact and } \epsilon > 1 + 1/d. \end{cases} \quad (24)$$

1315 Thus  $\epsilon$  can never “reach” the critical value  $\frac{d+1}{d}$  unless  $q$  is essentially bounded below on  
1316 its support.

1317  
1318 **From Nearest-Neighbour Distance to Approximation Loss**  
1319

1320 • Capped nearest-neighbour distance can be derived naturally if one assume the maximum  
1321 distance of neighboring points to be bounded by constant, or if one assume the Intrinsic  
1322 Space  $\mathcal{Z}$  is bounded.

1323 • **Restate of Theorem 2 in (Bahri et al., 2024):** Assuming  $l(f), f, F$  be Lipschitz with  
1324 constants  $K_L, K_f, K_F$  and  $l(F) = 0$ ,  $D$  be training dataset of size  $D$  sampled i.i.d from  
1325  $M_d$ . Let  $f(x) = F(x) \forall x \in D$ . Then, for each training point  $x$ , let  $\hat{x}$  be the nearest  
1326 neighboring training data point, we have  $L(D) \leq K_L(K_f + K_F)\mathbb{E}_{D,x}[\|x - \hat{x}\|]$ .

1327 • Combining **Theorem 2 in (Bahri et al., 2024)** and previous results (nearest neighbour  
1328 distance in this Appendix D.2), since Approximation loss of context length  $l$  is  $D_{KL}(P_l, Q)$   
1329 which can be 0 when  $Q = P_l$ , thus satisfying the assumption of **Theorem 2 in (Bahri et al.,**  
1330 **2024)**. Thus,  $L_{\text{Approx}} = C_0 + A(l)/D^{c/dim} = C_0 + A(l)/D^{\alpha(l)}$ .

1331 Therefore, we have:

1332 **Theorem 2** (Data Scaling for Approximation Loss). *Let  $\mathcal{Z} \subseteq \mathbb{R}^d$  ( $d > 1$ ) be a  $d$ -dimensional  
1333 region (exists non-empty open set  $U \in \mathbb{R}^d$  such that  $U \subseteq \mathcal{Z}$ ).  $q : \mathcal{Z} \rightarrow [0, \infty)$  be probability  
1334 density function satisfying **Lipschitz Differentiable** and **Finite  $\epsilon$ -negative moment**. Let  $g : \mathcal{Z} \rightarrow P_V$   
1335 be a decoding mapping from intrinsic space  $\mathcal{Z}$  to a distribution of tokens in vocabulary  $V$ , and  
1336  $l(P_{V1}, P_{V2})$  be KL divergence loss function (thus  $l$  is zero for identical distributions). Assume  
1337  $l(g(z_1), g(z_2))$  is differentiable and Lipschitz smooth for  $z_1$  and  $z_2$  with Lipschitz coefficient  $L_l$ .*

1338 *Then, draw i.i.d. samples  $\mathcal{Z}_D = \{Z_1, \dots, Z_D\} \sim q^{\otimes D}$ , if  $\min_{j \neq i} \|Z_i - Z_j\|$  is bounded by  
1339  $M$ , then there exists constant  $C = C(d, L, \epsilon, M, C_\epsilon, L_l)$  and  $c = c(L, \epsilon, M, C_\epsilon)$  such that for  
1340  $D > D_0(d, L, \epsilon, M, C_\epsilon)$ :*

$$\min_{j \neq i} l(g(Z_i), g(Z_j)) \leq C D^{-c/d}. \quad (25)$$

1345 *Proof.*

$$\begin{aligned} 1346 \min_{j \neq i} l(g(Z_i), g(Z_j)) &\leq \min_{j \neq i} L_l \cdot \|Z_i - Z_j\| \\ 1347 &= L_l \cdot \min\{M, \min_{j \neq i} \|Z_i - Z_j\|\} \\ 1348 &= L_l \cdot R_M(Z_i) \text{ by the definition of } R_M(Z_i) \text{ in Theorem 1} \end{aligned} \quad (26)$$

1350 By applying Theorem 1 we have:  
 1351

$$\mathbb{E}_{\mathcal{Z}_D} [\min_{j \neq i} l(g(Z_i), g(Z_j))] \leq L_l C D^{-c/d} \quad (27)$$

1354 for constant  $C = C(d, L, \epsilon, M, C_\epsilon)$ ,  $c = c(L, \epsilon, M, C_\epsilon)$  and large enough  $D > D_0(d, L, \epsilon, M, C_\epsilon)$ ,  
 1355 thus completing the proof.  $\square$   
 1356

1357 **Meaning of a finite  $\epsilon$ -negative moment**

1359 • **Lebesgue–measure view**

1360 Write  $E_t := \{z : q(z) \leq t\}$ . Chebyshev gives  
 1361

$$\text{Leb}(E_t) \leq t^{-\epsilon} \int q^{1-\epsilon} = C_\epsilon t^{-\epsilon}. \quad (28)$$

1362 Hence Assumption (A2) controls how *large* the very–low–density region can be; the  
 1363 smaller  $\epsilon$ , the larger that region may grow.  
 1364

1365 • **Rényi entropy view**

1366 For order  $\alpha > 0$ , the Rényi entropy is  
 1367

$$H_\alpha(q) = -\frac{1}{\alpha-1} \log \int q^\alpha. \quad (29)$$

1368 Setting  $\alpha = 1 - \epsilon \in (0, 1)$  (the *Tsallis* regime) and re-arranging,  
 1369

$$\int q^{1-\epsilon} = e^{-(1-\epsilon)H_{1-\epsilon}(q)}, \quad (30)$$

1370 so finiteness of the  $\epsilon$ -negative moment is equivalent to *finite sub-Rényi entropy of order*  
 1371  $< 1$ . Smaller  $\epsilon$  (order closer to 1) corresponds to heavier low-density tails, which precisely  
 1372 slows the nearest-neighbour rate as captured in Theorem 1.  
 1373

1374 D.3 DERIVATION FOR BAYES RISK WITH INTRINSIC DIMENSION ASSUMPTION  
 1375

1376 **Theorem 3** (Bayes Risk and Context Length with Intrinsic Dimension Assumption). *Let  $\mathcal{Z}$  be an*  
 1377 *intrinsic space satisfying **Predictive Consistency** and **Uniform Information Gain**, then the Bayes*  
 1378 *Risk  $H(P, P_l)$  of context length  $l$  is **Linear** with respect to Intrinsic Dimension  $\dim(l)$ . That is,*  
 1379

$$H(P, P_l) = -s \cdot \dim(l) + \text{Const} \quad (31)$$

1380 *Proof.*

$$\begin{aligned} H(P, P_l) &= H(P) + D_{KL}(P, P_l) \\ &= H(P) + s \cdot (\dim(\infty) - \dim(l)) \\ &= -s \cdot \dim(l) + \text{Const} \end{aligned} \quad (32)$$

1381  $\square$

1382 **An intuitive example for the ‘s-bits per dimension’ assumption:** assuming that the vocab is  
 1383 an integer from 0 to  $2^{\dim(\infty)*s} - 1$ . assuming  $P(x_0|x_{-\infty:0}) = \delta_{x_0,y}$ , that is, the next token  
 1384 given  $x_{-\infty:0}$  is sure to be  $y$ .  $y$ . For  $P_l(x_0|x_{-\infty:0})$ , the first  $\dim(l) * s$  digits of the integer  
 1385 (in binary representation) are known, but the remaining  $(\dim(\infty) - \dim(l)) * s$  digits are un-  
 1386 known, making a guess in these numbers yield  $P_l(x_0|x_{-\infty:0}) = 1/2^{s*(\dim(\infty)-\dim(l))}$ . Thus,  
 1387  $D_{KL,x_0}(P(x_0|x_{-\infty,0}), P_l(x_0|x_{-\infty,0})) = 1 * \log 1/(1/2^{s*(\dim(\infty)-\dim(l))}) = s * (\dim(\infty) -$   
 1388  $\dim(l))$ .  
 1389

1404 D.4 DERIVATION FOR BAYES RISK WITH INFORMATION ENTROPY ASSUMPTION  
1405

1406 **Theorem 4** (Bayes Risk and Context Length with Information Entropy Assumption). *Let  $\mathcal{Z}$  be  
1407 an intrinsic space satisfying **Predictive Consistency** and **Linear Entropy Relationship** of zero-  
1408 tolerance limit, then the Bayes Risk  $H(P, P_l)$  of context length  $l$  is **Linear** with respect to Intrinsic  
1409 Entropy  $H[q_t(\mathcal{Z})]$  where  $q_t(\cdot)$  denotes probability density function. That is,*

$$1410 H(P, P_l) = -s \cdot H[q_t(\mathcal{Z})] + \text{Const} \quad (33)$$

1411 *Proof.*

$$\begin{aligned} 1413 H(P, P_l) &= H(P_l) \text{ (from Appendix B.2)} \\ 1414 &= H[p(x_t | x < t)] \\ 1415 &= -s \cdot H[q_t(\mathcal{Z})] + b \\ 1416 &= -s \cdot H[q_t(\mathcal{Z})] + \text{Const} \end{aligned} \quad (34)$$

1417  $\square$

1419 E MORE EXPERIMENTS OF LLaMA ON ANOTHER DATASET  
1420

1421 According to the technical report of LLaMa 3.1(Grattafiori et al., 2024), the text corpora with number of ‘dirty words’ beyond certain threshold would be filtered out, as proposed in (Raffel et al.,  
1422 2023). We collect some text corpora online which include forbidden words defined in (Raffel et al.,  
1423 2023), as text corpora unseen by LLaMa 3.1. By conducting experiments on it we obtain results  
1424 similar to Openwebtext subset.  
1425

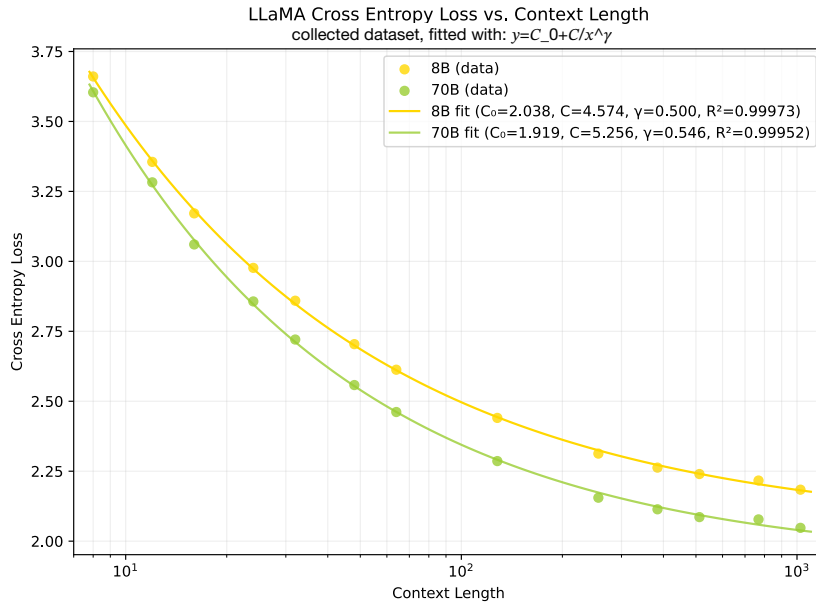


Figure 11: Cross Entropy Loss vs. Context Length, with log scale. We see that  $y = C_0 + C/x^\gamma$  fits this curve well.

According to Figure 11, we see that  $CE = C_0 + C/l^\gamma$  approximates well for text corpora that are sure not to be seen by the model.

F OPTIMAL CONTEXT LENGTH FOR TWO-NEEDLE-IN-HAYSTACK  
TRAINING: STUDY ON SYNTHETIC DATASET

Here, we utilize our proposed synthetic dataset as a proxy to study the two-needle-in-haystack experiment (as we mentioned in Figure 5.)

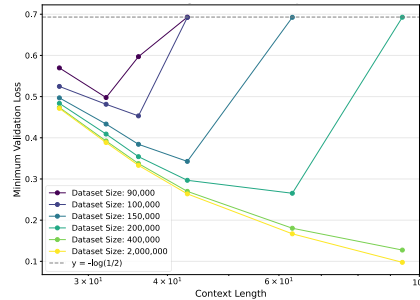


Figure 12: Validation set Cross Entropy Loss of the output token (resembling the ‘answer’ token of two-needle-in-haystack tasks) v.s. context length, for MLPs trained with different training dataset sizes.

As mentioned in previous studies, the Cross Entropy loss of key tokens (e.g. the perplexity of the Answer token for Needles in Haystacks (NIH)) is highly correlated with downstream task accuracy (that is, the NIH tasks). Here, we use the Cross Entropy loss of the output bit of our synthetic task (shown in Figure 5) as a metric for our synthetic ‘two-needles-in-haystack’ task.

Here, we use a synthetic dataset similar to that mentioned in the main paper, except that it has more than 500 context bits (though most tasks require only first 100 context bits). In this section, we fix the size of the training data, train multiple iterations till overfitting, and take the best validation loss as the validation loss of that (training dataset size, context length) pair. Results are shown in Figure 12. From the result, we make such observation:

There exists an optimal context length for most training dataset size used, and such optimal context length increases with the amount of available training data.

This proves the concept that, when training dataset is limited, optimal context length smaller than the task length could potentially exists for tasks resembling the two-needle-in-haystacks tasks, and larger training dataset leads to larger optimal context length.

## G EXPERIMENTS ON OTHER LANGUAGE MODELS

In our main paper, we mainly conduct experiments on the Llama-3 series on Nature Language and neural networks on synthetic datasets. Here, we further experiment on the relationship between Intrinsic Entropy and Cross Entropy Loss, for OpenWebText dataset for other two language models: the Qwen3-8B-Base and the RecurrentGemma-9B.

As shown in Figure 13, for Qwen3-8B-Base, the linear relationship between Intrinsic Entropy and Cross Entropy loss holds quite well. For RecurrentGemma-9B, we observe that its Cross Entropy loss is significantly higher than Llama-3.1-8B and Qwen3-8B-Base for small context length (the 3 high points drawn on the figure), while other points show similar cross entropy loss. Therefore, we conclude that **RecurrentGemma-9B is not a good approximation for Bayes Model for these outlier points (i.e. it can’t model low-context quite well with Cross Entropy loss > 5**, potentially because of its architecture or training pipeline), and we use the rest points where it is closer to Llama-3.1-8B and Qwen3-8B-Base as Bayes Model for regression.

Experiment in this section proves that, (1) our proposed Intrinsic Entropy and Cross Entropy loss relationship **holds across different series of Language Models with different architectures** when they are well-trained and can represent Bayes Models; and (2) the discovered relationship **only holds when the measured Language Model approximates Bayes Model well**.

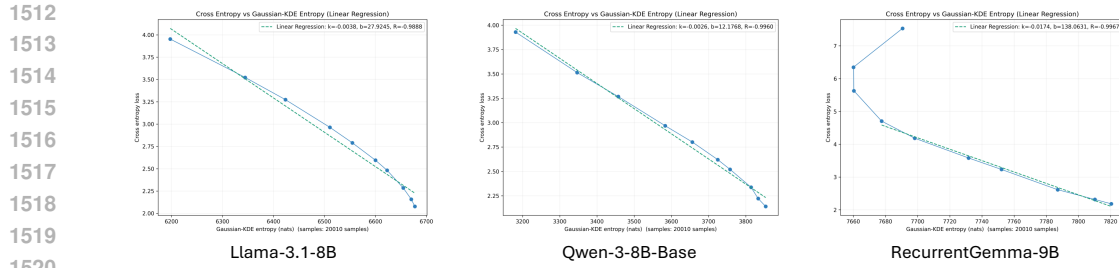


Figure 13: Validation set Cross Entropy Loss of the output token (resembling the ‘answer’ token of two-needle-in-haystack tasks) v.s. context length, for MLPs trained with different training dataset sizes.

## H EXPERIMENT SETTINGS

### H.1 NATURAL LANGUAGE DATA

#### H.1.1 OPTIMAL CONTEXT LENGTH EXPERIMENTS

We use nanogpt (Karpathy, 2022) and train a model with GPT-2(Radford et al., 2019) architecture on a subset of OpenwebText dataset. Our model is the same with GPT-2-124M (12-head transformers, 768-dim feature vector) except that it uses half the transformers layer size (12  $\rightarrow$  6) to reduce GPU memory for long contexts. For training, we use the AdamW (Loshchilov & Hutter, 2019) optimizer, learning rate of  $6e-4$ , weight decay of  $1e-1$ , 1000 warm-up iterations. For given token number, all models with different context length are trained with same number of iterations, where iteration number equals roughly to  $token\_number/(0.1M)$ .

We train the model on a subset of OpenWebText. To be specific, we first select text corpora with context length beyond specific limits larger than the maximum training context length from OpenWebText, then split into Training set and Validation Set. The training set we used to train the models have 200M, 250M, 300M, 350M, 500M, 750M tokens respectively, and the validation set has 134M tokens.

Experiments presented in Figure 4 and Figure 14 took around 300 gpu hours on 8 AMD MI-250X GPUs (which are similar in performance to Nvidia A100 gpus).

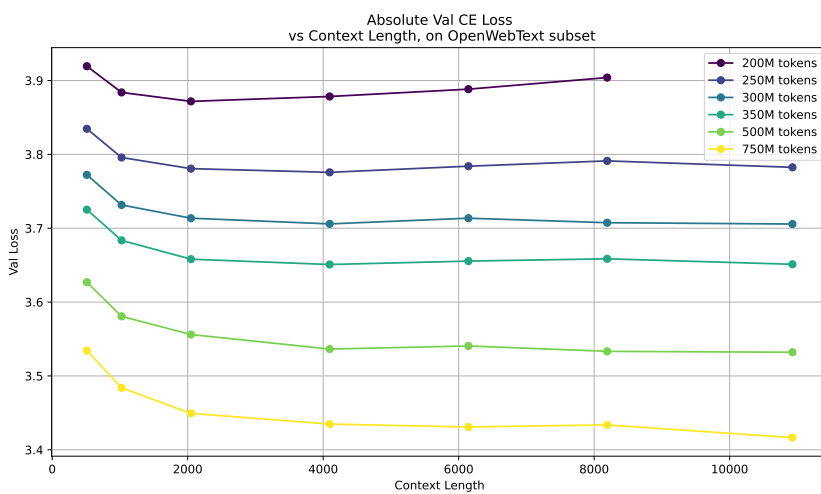


Figure 14: Openwebtext subset, Validation Loss vs. Context Length, for different dataset sizes. Different curves represent different amount of training data used. A more readable figure can be found in Figure 4, where the minimum validation loss reachable for each training dataset size is subtracted.

1566  
1567

## H.1.2 INTRINSIC DIMENSION EXPERIMENTS

1568  
1569  
1570  
1571

We select long enough text corpora from the Openwebtext dataset. Then, following previous practice (Cheng et al., 2023), we conduct experiments with LLaMa-3.1-8b on 10000 samples of this subset. We extract the feature representation of the last token in the last layer, as the Intrinsic Representation of samples.

1572  
1573

Conducting all intrinsic dimension measurements cost up to around 100 gpu hours for MI-250X gpus.

1574  
1575  
1576

## I RELATED WORK

1577  
1578

## I.1 ENLARGING CONTEXT LENGTH FOR LMs

1579  
1580  
1581  
1582

Previous work has made attempts to enlarge the context length of Language Models. Work represented by RoPE (Su et al., 2023) uses rotary positional embedding to support generalizing LMs to longer context in inference compared to the training process. These work uses modified positional embeddings to model the relative position dependency in attention mechanism.

1583  
1584  
1585  
1586

There is also work about enhancing long context understanding and exploring Scaling Laws for context length (Xiong et al., 2024). These work utilize an adjusted pretraining and instruction-finetuning process with more long-context data to enhance the models' ability on long contexts.

1587  
1588  
1589  
1590

Other work modifying architectures has also been proposed to enhance long context modeling or to simplify deployment of long context LLMs. For example, (Tang et al., 2024) proposes a training-free RazorAttention algorithm to largely compress the KV cache while maintaining performance unchanged.

1591  
1592  
1593  
1594  
1595

Architectures and inference methods have been proposed to reduce inference time and memory cost for Language Models, represented by a series of linear transformer or RNN-based methods (Katharopoulos et al., 2020; Gu & Dao, 2024; Sun et al., 2024). These methods, largely reducing the computational cost and memory usage for long input contexts, have displayed margin ahead of traditional attention-based langauge models for long context inference.

1596  
1597  
1598

Currently a common practice to train very large Language Models supporting long context is to use pretrain the model with shorter contexts, then finetune them with longer contexts, as presented in tech reports of LLaMa-3 (Grattafiori et al., 2024) and DeepSeek-v3 (DeepSeek-AI et al., 2024).

1599

## I.2 IRRELEVANT LONG CONTEXT HURTS PERFORMANCE OF LMs

1600  
1601  
1602  
1603  
1604  
1605  
1606  
1607

Besides context length scaling with relevant contexts, previous researches have studied how LLMs perform for long irrelevant contexts. As an example, (Levy et al., 2024) studies the performance of current LLMs on an adjusted version of ‘needle in a haystack task, where two pieces of key information are embedded into a long text corpora and a question related to both is asked, similar to that presented in Figure 5. The conclusion of these work is that LLMs would perform worse when there is too much irrelevant information.

1608  
1609

## I.3 LONG CONTEXT IN ANOTHER FIELD: TIME SERIES FORECASTING

1610  
1611  
1612  
1613  
1614  
1615  
1616

Context length, representing the length of input context, is not unique to Nature Language. For time series forecasting, where machine learning plays an important row, there is also work discussing the impact of context length, represented by (Shi et al., 2024). These investigations find that there exists an optimal look-back horizon, which increases with dataset size. However, time series datasets are relatively small compared to NLP datasets, and thus whether this conclusion holds on NLP remains an open problem for this work to study.

1617  
1618  
1619

Since the discovery of Scaling Laws for Large Language Models (Kaplan et al., 2020) or even earlier, there has been theoretical work trying to explain why model performance could benefit from

more data points and more model parameters. For example, (Sharma & Kaplan, 2022) studies the dataset and model scaling from the data manifold perspective.

Specially for Language Models, there is also previous work proposing all kinds of theoretical models. For example, (Michaud et al., 2024) proposes a feature-quant based theory; (Aghajanyan et al., 2020) views the effect of fine-tuning from the intrinsic dimension perspective; (Havrilla & Liao, 2024) proposes to understand scaling with intrinsic dimensions.

## J INTRINSIC DIMENSION PERSPECTIVE: MEASUREMENTS IN INTRINSIC SPACE

### J.1 BAYES RISK FROM AN INTRINSIC DIMENSION PERSPECTIVE: ASSUMPTIONS

Here we derive similar results as in Section 2.2, but from an Intrinsic Dimension perspective rather than an Information Entropy perspective.

We propose a simple theory model to relate  $H(P, P_l)$  with the intrinsic dimension  $\dim(l)$  of the intrinsic space  $\text{space}_l$  of the text corpora of length  $l$  (for the next-token prediction task).

We assume these assumptions hold for Intrinsic Space (please see formal definitions of Intrinsic Space in Appendix D),

- Assumption 1. Intrinsic Dimension of the Bayes Model  $\lim_{l \rightarrow \infty} \dim(l) = \dim(\infty)$  is finite, which is the Intrinsic Dimension of next token prediction of language itself.
- Assumption 2.  $\forall l_1, l_2$  such that  $l_1 < l_2$ ,  $\dim(l_1) < \dim(l_2)$ . This is because a longer context contains more information about the next possible token.

To simplify deduction, we further assume that,

- Assumption 3. **Uniform Information Gain** ( $s$ -bits for next token prediction per Intrinsic Dimension): Each intrinsic dimension would add  $s$  bits of information to the next-token prediction task, so there are  $\dim(l) * s$  bits of information that can be represented in  $\text{space}_l$  for the next-token prediction. This means the KL-divergence for the Bayes Model of context length  $l$ ,  $P_l$ , with Bayes Model of infinite context length,  $P = P_\infty$ , is:  $D_{KL}(P, P_l) = s * (\dim(\infty) - \dim(l))$ . **Note this does not mean these are the only information in the Intrinsic Space, hence  $s$  can be small, or even smaller than 1.**

With these assumptions, we can derive  $H(P, P_l)$  with  $\dim(l)$ :

$$\begin{aligned} R_{Bayes} &= H(P, P_l) \\ &= -s * \dim(l) + Const \end{aligned} \tag{35}$$

This **linear relationship** can be observed in experiments for LMs and synthetic data, providing an alternative explanation to the entropy-based approach in the main paper.

### J.2 EXPERIMENTALLY MEASURE INTRINSIC DIMENSION USING PCA

We further use PCA as a metric to measure the Intrinsic Dimension of Dataset with respect to context length. We provide the relative degradation of the eigenvalue in the feature space of LLaMa-3.1-8B, for the last token. We see that larger input length would indeed provide feature with lower degradation in the intrinsic space. Notably, when  $5 < \text{idx} < 1500$  the curves is similar to Zip-f distribution ( $\log \text{eig} = C_0 - C * \log \text{idx}$ ), and for  $500 < \text{idx} < 4000$  it resembles exponential degradation ( $\log \text{eig} = C_0 - C * \text{idx}$ ).

Instead, following previous practice, here we use some **threshold** to decide the transformation index of these two states as Intrinsic Dimension:  $\max_{\text{idx}} \text{rela\_eig}(\text{idx}) \geq \text{threshold}$  is used as the measured **Intrinsic Dimension**. Notably, the threshold here is a hyperparameter which is set to constants in previous work(e.g.1/20 in (Aghajanyan et al., 2020)), but we observe here that many thresholds would validate the linear correspondence of Cross Entropy vs. Intrinsic Dimension, which further enhance the robustness of our result. We use thresholds from 0.002 to 0.25.

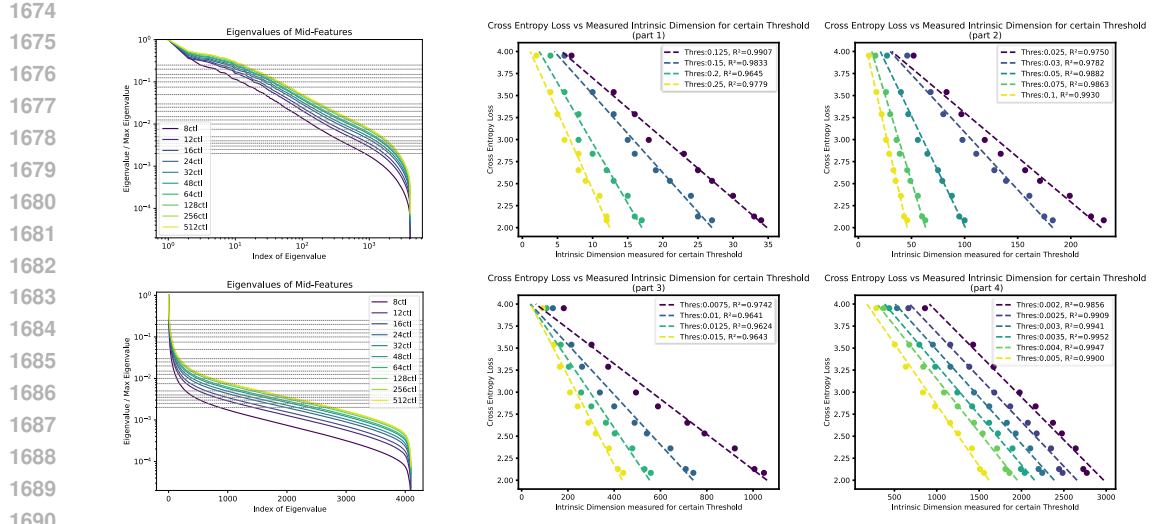


Figure 15: **Left figures: Relative Eigen Value** for LLaMa-3.1-8B on a subset of OpenWebText, presented in different x-axis scales, with different context length visible to Language Model. Gray lines represent different **thresholds** we take to measure the intrinsic dimension of the current model. **Right figures: Cross Entropy Loss vs. Measured Intrinsic Dimension.** Each line represents a certain threshold used to measure ID in the intrinsic space of the used LLM. Different Measurements would give ID values that are linear w.r.t. each other, and they are all linear w.r.t. CE loss.

For a certain threshold, we conduct experiments on several context lengths, and measure CE Loss on certain text corpora with these context lengths. We observe a fairly linear relationship between CE Loss and ID measured (supporting our theory), as shown in Figure 15. We see that, no matter what threshold we use, the Cross Entropy Loss usually follows a linear relationship with the Intrinsic Dimension we measured, showing the robustness of the PCA evaluation method, and validating our theoretical assumptions:

$$R_{Bayes} \approx -s * \dim(l) + Const,$$

which aligns well with **Equation 35**, thus validating our intrinsic dimension-based deduction.

### J.3 MLP-BASED SYNTHETIC DATASET: INTRINSIC DIMENSION EXPERIMENTS

We train a large enough MLP on data generated on the synthetic tasks, and evaluate our model on the validation dataset. We train until overfitting the training dataset. We assume 1 dimension in Intrinsic Space can store information about 1 subtask, hence we take  $ID(l) = t(l)$  as its theoretical value here.

Let  $f(x, C, C_0, \gamma) = C_0 - C/x^\gamma$  and  $g(x, k, b) = k * x + b$ .

The fitted results are:

- ID & CL:  $ID \approx f(CL, C, C_0, \gamma), C_0 = 51.1 \pm 1.0, C = 1.7 * 10^3 \pm 0.3 * 10^3, \gamma = 1.18 \pm 0.06, R^2 = 0.9997$ .
- CE & CL:  $CE \approx f(CL, C, C_0, \gamma), C_0 = -0.015 \pm 0.013, C = -23.8 \pm 4.3, \gamma = 1.18 \pm 0.06, R^2 = 0.9997$ .
- CE & ID:  $CE \approx g(ID, k, b), k = -0.693 \pm 1 * 10^{-5}, b \approx 0.0139 \pm 4 * 10^{-7}, R^2 = 1 - 7 * 10^{-9}$ .

As shown, we construct synthetic data such that  $ID(l) = ID_0 - C'/l^\gamma$ , and our measurements show  $CE = C + C'/l^\gamma$ . More importantly, **for the synthetic data example, Cross Entropy loss is almost perfectly linear with the Intrinsic Dimension as we defined previously.** This validates the linear relationship between Cross Entropy Loss and Intrinsic Dimension; and we have also provided a construction to match the measured relationship  $CE(l) \approx C_0 + C/l^\gamma$ .

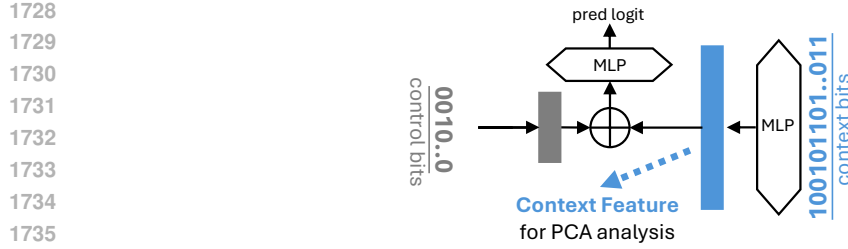


Figure 16: Model trained on the proposed synthetic dataset;  $\oplus$  represents feature concatenation. Only the first  $l$  bits are used as input to context MLP when the context length is set to  $l$ . We conduct PCA on Context Feature to analyze the intrinsic dimension of input context bits for various context lengths.

We train a model with a specialized architecture, allowing us to use the feature representation of a middle layer as a feature vector for input context bits, as shown in **Figure 16**. After training the model on data with different context length, we conduct PCA on the obtain context feature representation to study the Intrinsic Space of this model.

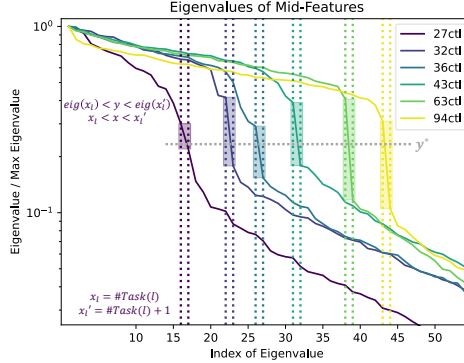


Figure 17: Relative eigen value vs. index, for models trained on different context length. Vertical lines:  $x_l = ID(l)$  and  $x'_l = ID(l + 1)$ . For example, a context length 27 has 16 subtasks visible, corresponding to 16 bits in Intrinsic Space. Assuming 1 dimension in Intrinsic Space represents 1 bit, the leftmost purple rectangle drawn means a range of  $y_{threshold}$  that would provide an accurate estimation of  $ID(27) = 16$  for context length 27. There exists  $y^*$  that would provide an estimation of  $ID$  for all context lengths, as shown in the figure.

We find that: (1) the neural network would indeed learn the key information in the context bits. For models with different input context lengths, although their inner dimensions are the same (80), the representation of inputs in this inner space mainly lies in the first  $ID$  dimensions, and the eigen values corresponding to other dimensions are very small; and (2) there exists such threshold  $y^*$  that would estimate  $ID$  for all context lengths accurately. We can take some threshold  $y^*$  to estimate the intrinsic dimension, by obtaining the maximum index of the relative eigen value such that the relative eigen value is larger than  $y^*$ , which would give accurate and consistent estimates.

#### J.4 BRIDGING THE GAP BETWEEN INTRINSIC DIMENSION EXPLANATION AND INTRINSIC ENTROPY EXPLANATION

Here, starting from previous assumptions and measurements w.r.t. Entropy in Intrinsic Space, we explain why CE is linear w.r.t. Intrinsic Dimension measured in Section 2.2, for  $idx > 500$ . We see in Figure 3 that for  $idx > 500$ , the relative eigenvalues mainly follow an exponential decay:

$$releigval_{l, idx} = releigval_{l, 0} * \exp\{-\alpha_l * idx\}, \text{ for certain context length}$$

1782 where  $l$  is the context length,  $idx$  is the index of some certain eigen value, and  $\alpha_l$  is the exponential  
 1783 decay coefficient for this certain context length  $l$ .

1784 We also see from the previous results (**Figure 3**) that for different context lengths, the relative  
 1785 eigenvalues increase almost in the same proportion, especially for  $idx > 1000$ . That is,  $\alpha_l \approx \alpha$ . We  
 1786 define  $\gamma(l) = \text{releigval}_{l,0}/\text{releigval}_{\infty,0}$  and thus we have:  $\text{releigval}_{l,0} = \text{releigval}_{\infty,0} * \gamma(l) * \exp(-\alpha * idx)$ .

1787  
 1788 For the subspace for the next token prediction task, we denote its dimension to be  $m$ . Hence, the  
 1789 entropy should be proportional to log of volume in the subspace; that is:

$$1791 \quad S_{\text{subspace}}(l) = \sum_{idx \in \{\text{dimension of subspace}\}} \log \text{releigval}_{\infty,0} \gamma(l) \exp(-\alpha * idx) \quad (36)$$

$$1792 \quad = m \log \gamma(l) + \text{Const}$$

$$1793$$

$$1794$$

1795 which is the result of the **Intrinsic Entropy Explanation**.

1796 For **Intrinsic Dimension explanation**, if we are using some certain threshold  $thres$  to measure  
 1797 Intrinsic Dimension, the measured dimension  $\text{dim}(l, thres)$  should satisfy:

$$1800 \quad \text{releigval}_{\infty,0} * \gamma(l) * \exp\{-\alpha * \text{dim}(l, thres)\} = thres,$$

$$1801$$

1802 hence the measured dimension is  $\text{dim}(l, thres) = 1/\alpha * (\log \gamma(l) + \log(\text{releigval}_{\infty,0}/thres))$ .  
 1803 Plugging this into Equation (36) we have:

$$1804 \quad L_{CE} = -S_{\text{subspace}}(l) + \text{Const} = -m\alpha * \text{dim}(l, thres) + \text{Const}(thres). \quad (37)$$

$$1805$$

1806 Thus, we derive our assumptions in Section 2, where  $s = m\alpha$ . Equation (37) can also be validated  
 1807 in the lower-right part of Figure ??, where the Intrinsic Dimensions (for  $idx \geq 500$ ) are measured in  
 1808 the exponential decay area, and these lines, though measured with different threshold ( $thres$ ), share  
 1809 similar slopes w.r.t. CE Loss (that is not related with threshold, as shown in Equation 37).

## 1811 K DISCLOSURE OF LLM USAGE

1812 LLMs are used in this work for polishing writing only.

1813  
 1814  
 1815  
 1816  
 1817  
 1818  
 1819  
 1820  
 1821  
 1822  
 1823  
 1824  
 1825  
 1826  
 1827  
 1828  
 1829  
 1830  
 1831  
 1832  
 1833  
 1834  
 1835